EXPLORATION FOR
A GEOTHERMAL SYSTEM IN THE
LUALUALEI VALLEY, OAHU, HAWAII

by

M. Tahsin Tasci

A Thesis submitted to the Faculty and the Board of Trustees of the Colorado School of Mines in partial fulfillment of the requirements for the degree of Master of Science, Geophysical Engineering.

Signed: M. Tahsin Tasci
M. Tahsin Tasci

Golden, Colorado

Date: Mar. 14, 1975

Approved: George V. Keller
George V. Keller
Thesis Advisor and
Head of Department

Golden, Colorado

Date: Mar. 14, 1975

ABSTRACT

Lualualei Naval Magazine is located in the northeastern corner of the Lualualei Valley, Oahu, Hawaii. It has an area of approximately 12 square miles between latitudes 21°29' and 21°24'25" north and between longitudes 158°09' and 158°05'45" west. The elevation of the area of interest is about 250 feet above sea level with a gentle westward slope. Shear cliffs of the Waianae Range bound the area to the north, east and south, and alluvial plains of the Lualualei Valley extend all the way to the Pacific Ocean to the west.

In the last three weeks of September 1974, a detailed rotating-quadripole study was carried out. The purpose was to determine the possibilities of discovering a geothermal system in the area by mapping the lateral resistivity variations. Anomalously low resistivities were encountered to the southwest of the area in the vicinity of the Magazines #11 and #12. To make sure that the low resistivities were not caused by saturated alluvial fill (high clay content) or possibly by saline water at depth, shallow (1 meter) temperature measurements and a self-potential study were made in the last week of November 1974. Contoured temperature values showed that the area with anomalous resistivities (less than 30 ohm-m) had a temperature of 26.3°C, and the areas with high resistivities (75 ohm-m or higher) had an average temperature of 24.6°C, in general. A temperature difference of about 2°C is

believed to be anomalous. Contoured self-potential values did not show a pattern.

Even though the island of Oahu has been studied extensively by geologic and geophysical methods, no detailed geophysical work was done in this area. Previous studies by other investigators have included a gravity and aeromagnetic study of the whole island, deep electrical soundings on the northwestern part of the island, seismic studies using well-logging, refraction, and reflection methods in the Ewa Coastal Plain, and on shore and off shore seismic refraction surveys.

Presence of a heat source, a reservoir rock, abundant groundwater, and partially consolidated alluvium which could behave like a cap rock in the area suggests the presence of a geothermal system. Anomalous low resistivities and high temperatures in the same area increases the possibilities of high enthalpy water (higher than 200°C) at an economical depth (less than 10,000 feet).

It is believed that a shallow hole, deep enough to penetrate the basalt below the alluvium, should be drilled for a more conclusive evaluation of the prospect.

CONTENTS

ILLUSTRATIONS

Figure | Page

Table

ACKNOWLEDGMENTS

I am thankful to Dr. Norman Harthill of Group Seven, Incorporated for introducing me to the field of geothermal exploration. I sincerely appreciate Dr. Takashi Ohya's and Robert Crewdson's help in collecting the field data, without their help I would probably still be in the field.

My special thanks go to Dr. George V. Keller for making this project possible; his suggestions, ideas, and encouragement during the course of this study. I also thank Dr. L. T. Grose for doing the initial geological investigation of the area.

INTRODUCTION

The current energy crisis demonstrates that it is time to look for new sources of energy, such as geothermal, nuclear and solar. Geothermal reservoirs often derive their heat from magma; therefore, they are considered to be nearly inexhaustable sources of energy. They are environmentally acceptable. Besides being a source for electrical power, the energy can be used directly for space heating, industrial and agricultural purposes. Because of these reasons, attention given to geothermal exploration has been widespread and increasing in recent years.

Hot springs were used for heating, agricultural and recreational purposes long before the 20th century. Italy was the pioneer in using geothermal steam to produce electricity (1904). Italy was followed by New Zealand, Mexico, Iceland, Central America, and the United States. Not only the governments of these countries, but private companies and other organizations have been interested in geothermal exploration. For example, this study was sponsored by the Navy of the United States.

Geothermal exploration is in its initial development. All the fields currently exploited or under development have been found by drilling near areas of surface activity, the original discovery of which owes nothing either to geology or to geophysics (Banwell, 1970). The selection of areas where geophysics and geology were used has been strongly biased towards obvious surface activity. It may be too early to set up rules and use analogies in geothermal exploration, but that is one way of making use of the work that has been done so far.

Geothermal systems are defined as particularly hot areas of the earth's crust and where upward water circulation permits extraction and utilization of energy from depth. Their geologic environments have been classified a number of ways by different authors. The classification given by McNitt (1970) had three divisions; Quaternary volcanic centers, fields associated with Cenozoic tectonism, and fields in foreland and platform regions. It should be noted that these divisions do not draw definite lines between two environments. One type could be found grading into the next and sharing its characteristics. For example volcanic structures are often superimposed on purely tectonic structures.

The islands of Hawaii are shield-shaped basaltic domes; therefore, thermal water on these islands owes its heat to volcanic sources. It may well be that the rocks in Hawaii are too permeable to permit steam to accumulate under pressure at levels close to the surface, and the abundance of cold ground water makes unlikely the occurrence of steam at a temperature appreciably above the boiling point (MacDonald and Abbott, 1970). A borehole was drilled at the summit of Kilauea Volcano during the summer of 1973 (Keller, 1974). It appears that commercial quality steam could be obtained at a practical depth. Undoubtedly, a tremendous amount of volcanic heat exists at relatively shallow depths in the islands of Hawaii.

The Waianae caldera on the island of Oahu is a late Tertiary volcanic center which exhibited resurgent activity during Quaternary period. The study area is located in the Lualualei Valley which is situated to the west of the Waianae Range (see Figs. 1 and 2). Despite the possibility of existence of a heat source, there are no geothermal surface manifestations such as geysers, hot springs, fumaroles, solfatras, etc. Considering the conditions given above, this geophysical investigation was directed to study the area for a buried geothermal system.

A review of geophysical and geologic work done previously by other groups was made. Gravity, magnetic and seismic information helps define the geologic environment of the study area and its relationship to the volcanic center and the rift zones.

Electrical resistivity methods have been successfully used to locate geothermal reservoirs in different parts of the world for a number of years (Keller, 1970). In order to cover the area in detail and in a short period of time the dipole mapping technique (Furgerson, 1970; Keller, et al, 1974) was chosen as the main exploration technique. This technique is very effective in mapping lateral resistivity variation and gives a general idea of the vertical variations. Use of one dipole source is not enough to determine best

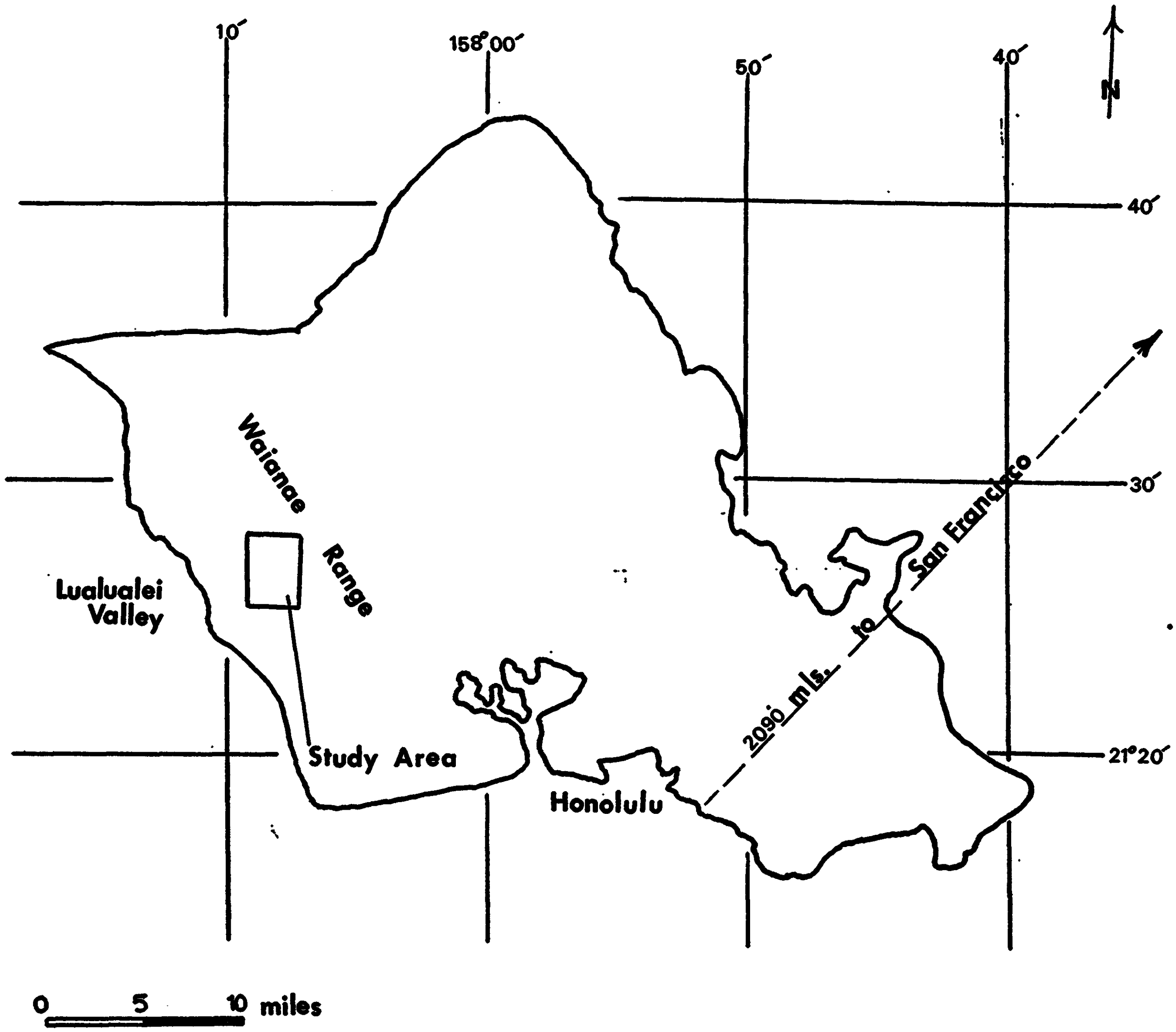

Figure 1. Map of Oahu showing location of the study area.

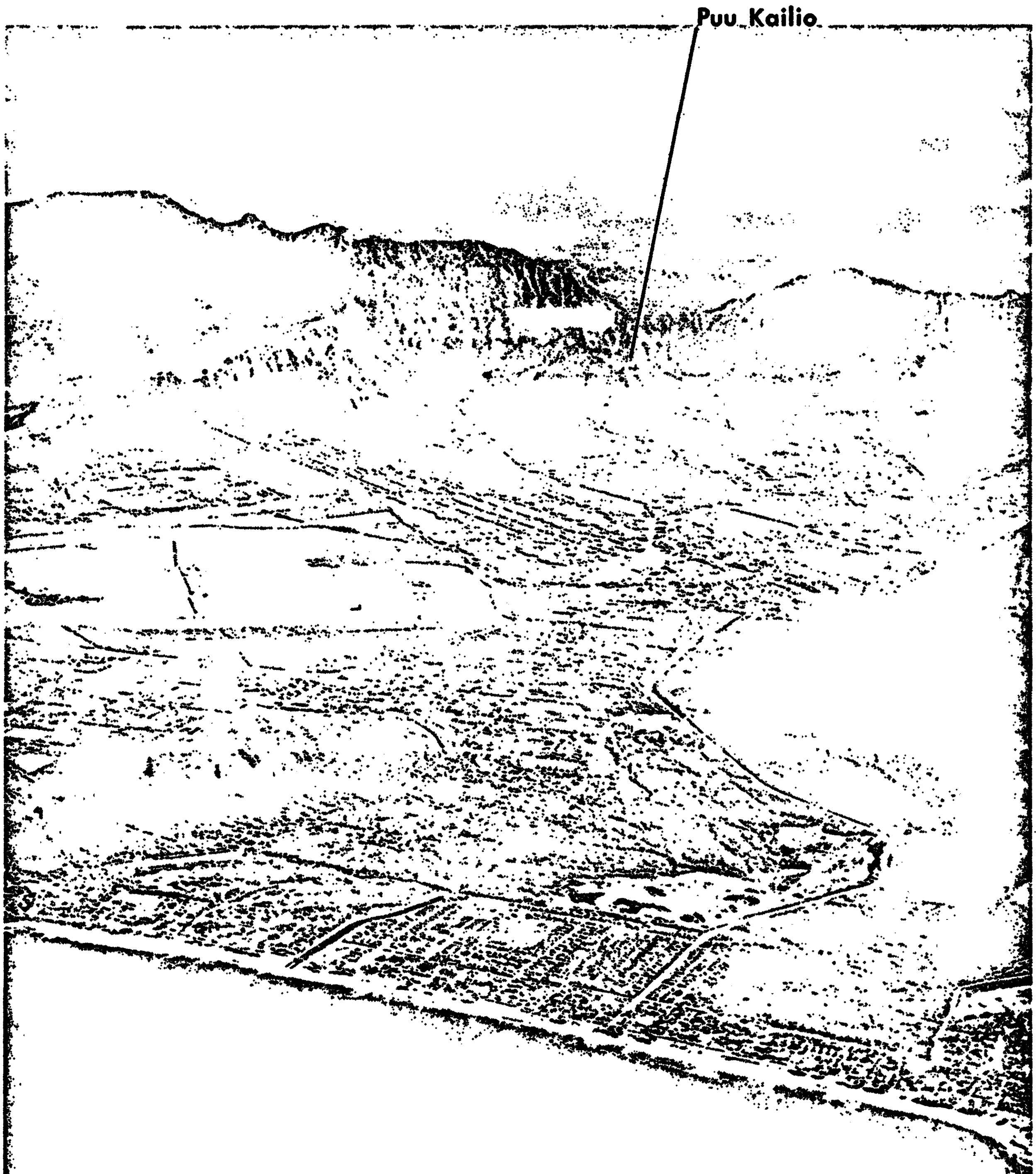

Figure 2. Picture of the Lualualei Valley showing location of the study area (after Macdonald and Abbott, 1970).

apparent resistivities and anisotropies can cause false anomalies (Keller, et al, 1975). In order to eliminate the possibility of observing a false anomaly, two dipole sources at about right angles to each other were set up in the same area. Data from both of these sources were treated together using the rotating-quadripole method to compute the best apparent resistivities. The purpose was to delineate an area with low resistivities, inasmuch as geothermal reservoirs contain water and steam at high temperatures and pressures and dissolved salts; they have higher conductivities than the surrounding rocks.

During the surveys, a relatively conductive zone was discovered. A shallow temperature study was carried out and the results correlated well with the rotating-quadripole data, increasing the likelihood of there being a sealed geothermal reservoir present.

GEOLOGY OF THE AREA

General Statement on the Hawaiian Islands

The Hawaiian Islands are a chain of basaltic shield volcanoes built over a fissure 1600 miles long in the ocean floor between 154°40' and 171°75'W longitude and 18°54' to 28"15'N latitude. Recent gravity, magnetic and seismic studies convincingly showed that the lavas which built the Hawaiian islands were extruded primarily along faults oriented either east-west and associated with the Molokai fracture system or northwest-southeast and associated with the trend along which lie the Koolau dike complex and the Musician Seamounts. The volcanic pipes may have formed at points of intersection of rifts of the two fracture systems. Whether the NW-SE fracture system is a strike-slip fault, a simple tension crack or a tear along the crest of a fold is not known. To the southwest of Honolulu at about 1700 feet below sea level, some fossils and shallow-water corals of late Miocene age were discovered (MacDonald and Abbott, 1970). Therefore, the Hawaiian Islands might have been built on an older ridge, perhaps contemporaneous with a chain of islands that existed in middle and early Tertiary time further northwest. The NW-SE fracture system probably has been existent since early Tertiary (Stearns, 1966).

The Hawaiian Islands were built by extrusive materials from volcanic centers during late Tertiary and Quaternary

The weight of the extruded lavas caused the ridge to sink in order to reestablish isostatic equilibrium. Since the depth to Moho is about 15 km on the Ridge and about 11 km in the normal ocean basin, a thickening of the crust of some 4 km is indicated (Strange, Woollard, and Rose, 1964). Along with volcanism, erosion has taken place. Sea cliffs and drainage systems have been developed. The islands have continued to submerge. The older islands to the northwest are believed to have submerged up to about 9000 feet (Stearns, 1966). Concurrently, a new epoch of volcanism began and secondary outbreaks continued into Recent time. The eruptions occurred on all the major islands except Lanai in Quaternary period. Complex submergences and emergences continued. Because of the rapid alterations of these events very little reef formation took place.

Recently drilled wells in Lualualei Valley penetrated 1200 feet of stream-deposited alluvium before entering lava rock. Since the bottom of the valley is 1200 feet below sea level and the valley had to be cut above sea level, it was concluded that the island must have sunk at least 1200 feet since the alluvium was deposited (MacDonald and Abbott, 1970).

General Statement on the Geology of Oahu

Oahu is a volcanic doublet with an area of 604 square miles and has four major geomorphic provinces. They are: 1) Koolau Range, 2) Waianae Range, 3) Schofield Plateau, and 4) Coastal Plain (see Figure 3).

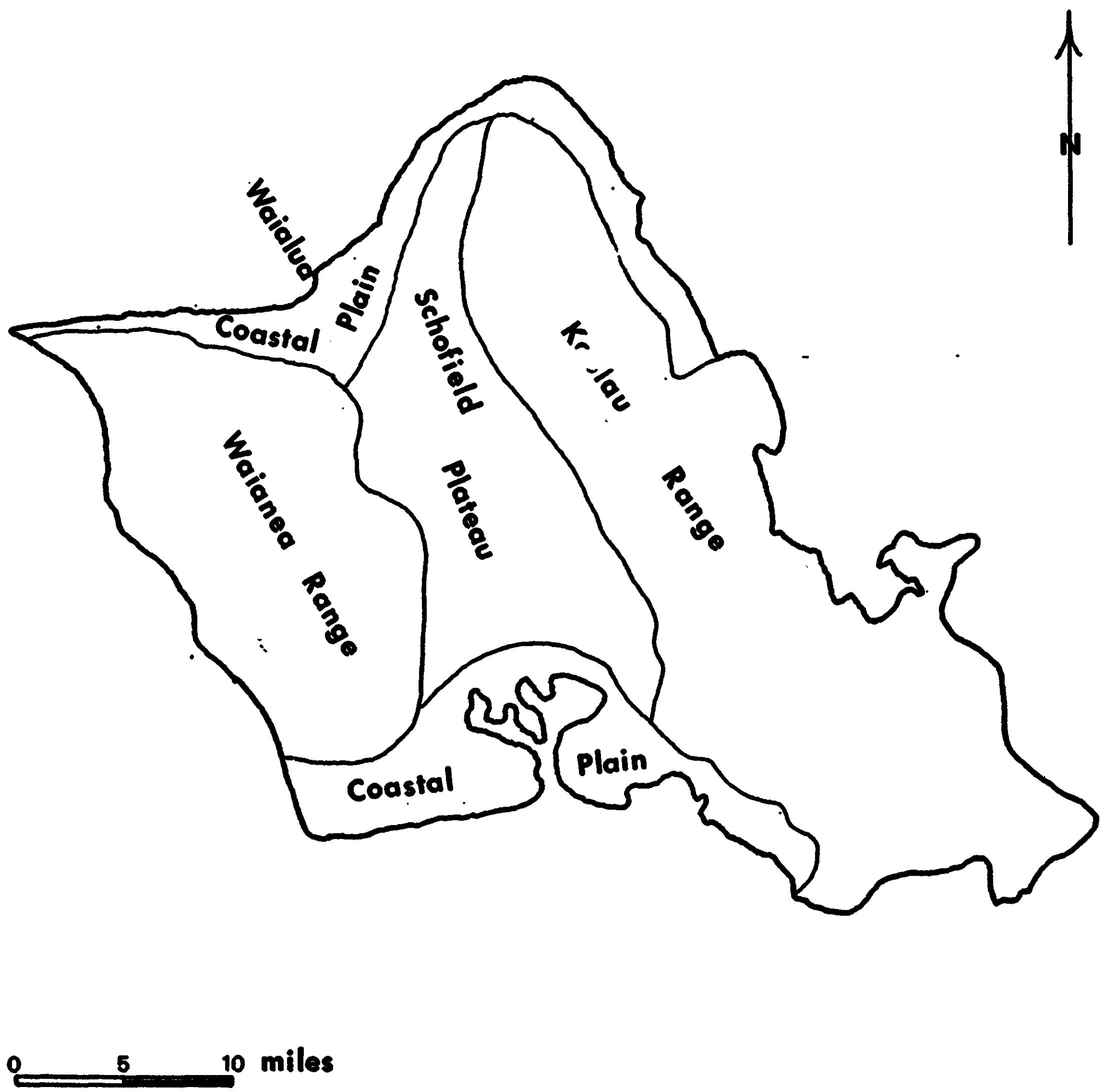

Figure 3. Map of Oahu, showing the major geomorphic provinces (after Stearns, 1966).

The Koolau Range is the younger of the two ranges on the island and it is located to the east. It was built principally by eruptions along a northwest-trending rift zone. The rocks of the Koolau Volcano are mainly tholeiitic basalts and olivine basalts with small amounts of oceanite. They have been divided into two groups. The Kailua Volcanic series are the eroded rocks of the ancient Koolau caldera. These rocks are altered by hydrothermal action due to steam rising in the vent area. The Koolau volcanic series are those lavas and dikes lying outside the caldera and are altered only rarely by hydrothermal action. After the Koolau volcano ceased activity, a period of erosion and deposition started lasting about 2 million years. Then volcanic activity resumed on the southeastern end of the Koolau range. About 30 vents have erupted and they are called the Honolulu volcanic series. The vents are aligned chiefly along NE-SW fissures and the lavas include nephelinites, basanites, and alkalic olivine basalts.

The Waianae Range is located to the west of the island. The Waianae Volcanic series, erupted in Tertiary time, is divided into lower, middle and upper members. The lower member built the main mass of the Waianae shield volcano. It comprises the tholeiitic lava flows and associated pyroclastic rocks. The middle member consists of tholeiitic rocks that accumulated in the caldera, gradually filling it. Alkalic basalts begin to appear toward the top of the middle member. The upper member is the relatively thin cap that appears to have covered the entire top of the shield late in its history. It is largely hawaiite with lesser amounts of alkalic olivine basalt. See Table 1 for stratigraphic rock units and their ages (Stearns, 1966). Some posterosional eruptions occurred on the Waianae Range, during the Pleistocene, near the ancient caldera. These alkalic olivine basalts are called Kolekole volcanics and they are probably correlative with the secondary eruptions on the Koolau Range.

The Schofield Plateau was formed by the lavas from the Koolau Range banking against the already-eroded slope of the Waianae Volcano to form the gently sloping surface of the Schofield Plateau. An erosional unconformity between the rocks of the two volcanos is visible along Kaukonahua Gulch at the eastern foot of the Waianae Range (MacDonald and Abbott, 1970).

The coastal plain lies mostly on the ponded lavas of the Koolau Volcano north and south of the Schofield Plateau. The plain is composed mainly of marine sediments deposited on the lavas when the sea stood higher in mid-Pleistocene time. See Figure 4 for the geologic map of the island of Oahu.

Geology of the Study Area

After the Waianae Volcano ceased activity, stream erosion began and great valleys were carved, especially on the southwest side of the Waianae Range where the streams were older and the rocks weaker. Then the island went through a complex cycle of submergences and emergences (Stearns, 1966). The

Table 1. Stratigraphic rock units in the island of Oahu (after Stearns, 1966).

Age	Waianae Range	Koolau Range
Historic	Coral fill	Coral fill
Recent	Younger alluvium and consolidated calcareous beach and dune deposits	Younger alluvium, unconsolidated beach and dune deposits, and younger rocks in the Honolulu volcanic series
	Local Unconformity	
Pleistocene	Lithified calcareous dunes, emerged marine limestone, older alluvium, and Kolekole volcanics	Lithified calcareous dunes, emerged marine limestone, older alluvium, and older rocks in the Honolulu volcanic series
	Great Erosional Unconformity	
Pliocene and Older	Waianae volcanic series; upper, lower and middle members	Koolau and Kailua volcanic series

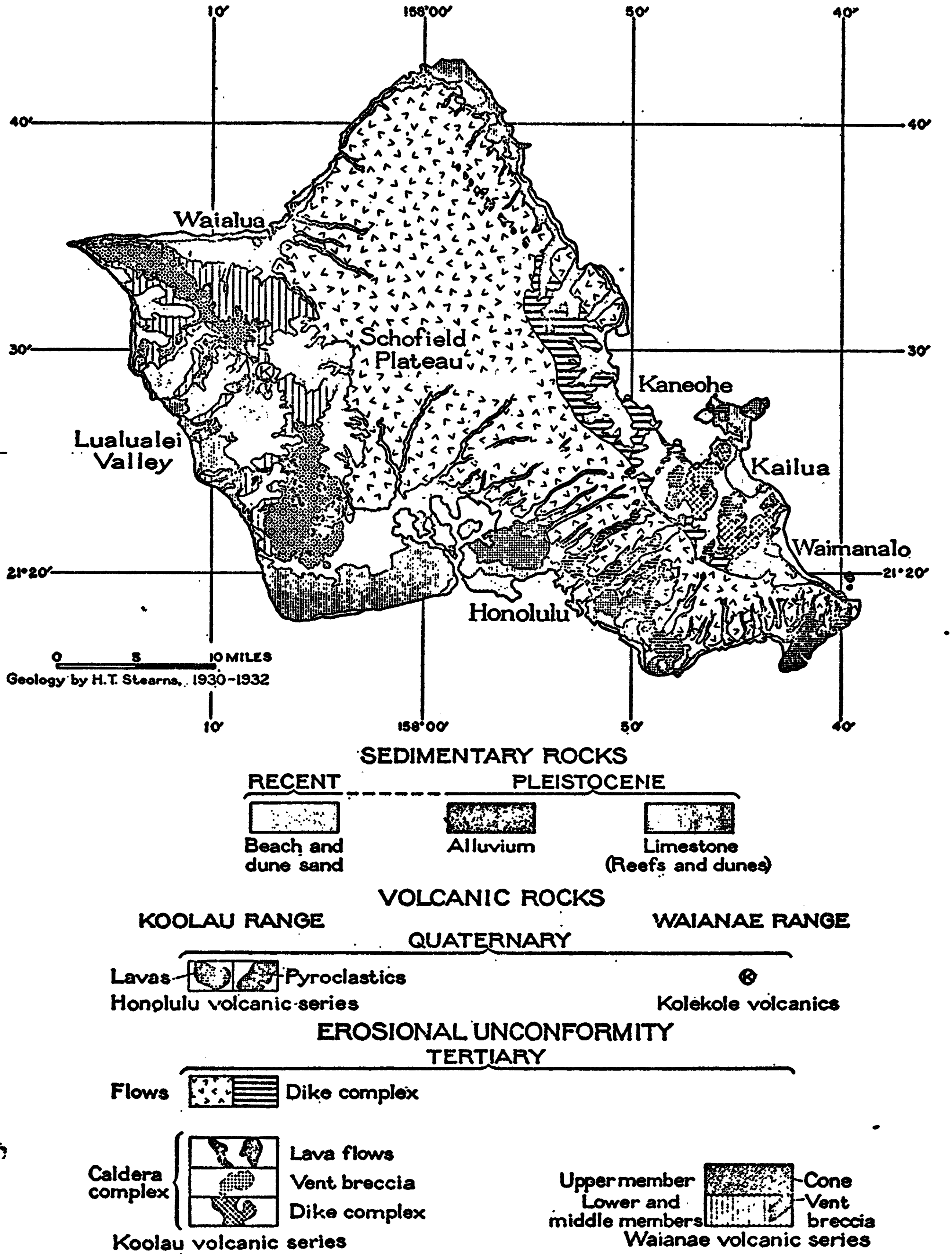

Figure 4. Geologic map of the island of Oahu (after Stearns, 1946)

great submergence resulted in deep drowning of the great valleys and their subsequent sedimentation. Re-emergence of Oahu exposed the great valleys to erosion once more, with their nearly flat alluvial plains. The area is located at the northeast corner of one of these valleys, namely the Lualualei Valley.

The study area is covered with alluvium. The exact thickness of alluvium in the vicinity of the anomaly is not known; however, it is believed to be about 1200 feet (probably less than 1200 feet), since drill holes penetrated 1000 feet of alluvium near the town of Waianae and 1200 feet in the Lualualei Valley (MacDonald and Abbott, 1970). It is expected to get thinner towards the steep walls of the valley, to the east, the north and the south. Outcrops in the eastern and the northeastern part of the area are believed to be from the Lower Member of the Waianae Volcanic Series. Kolekole volcanics which was the result of renewed volcanism in the Pleistocene time is located three miles to the northeast of the anomaly (Fig. 4). The caldera of the Waianae Volcano was located in the area immediately west of Kolekole Pass, and extended from the northern side of Makaha Valley to the head of Nanakuli Valley (Fig. 5). This puts the study area close to the center of the caldera. Near the area where the Lower and the Middle members of the Waianae Volcanic Series are exposed, there are numerous dikes. Their sizes vary between a few inches and 15 feet, and most of them are nearly vertical with a general trend parallel to the rift zones.

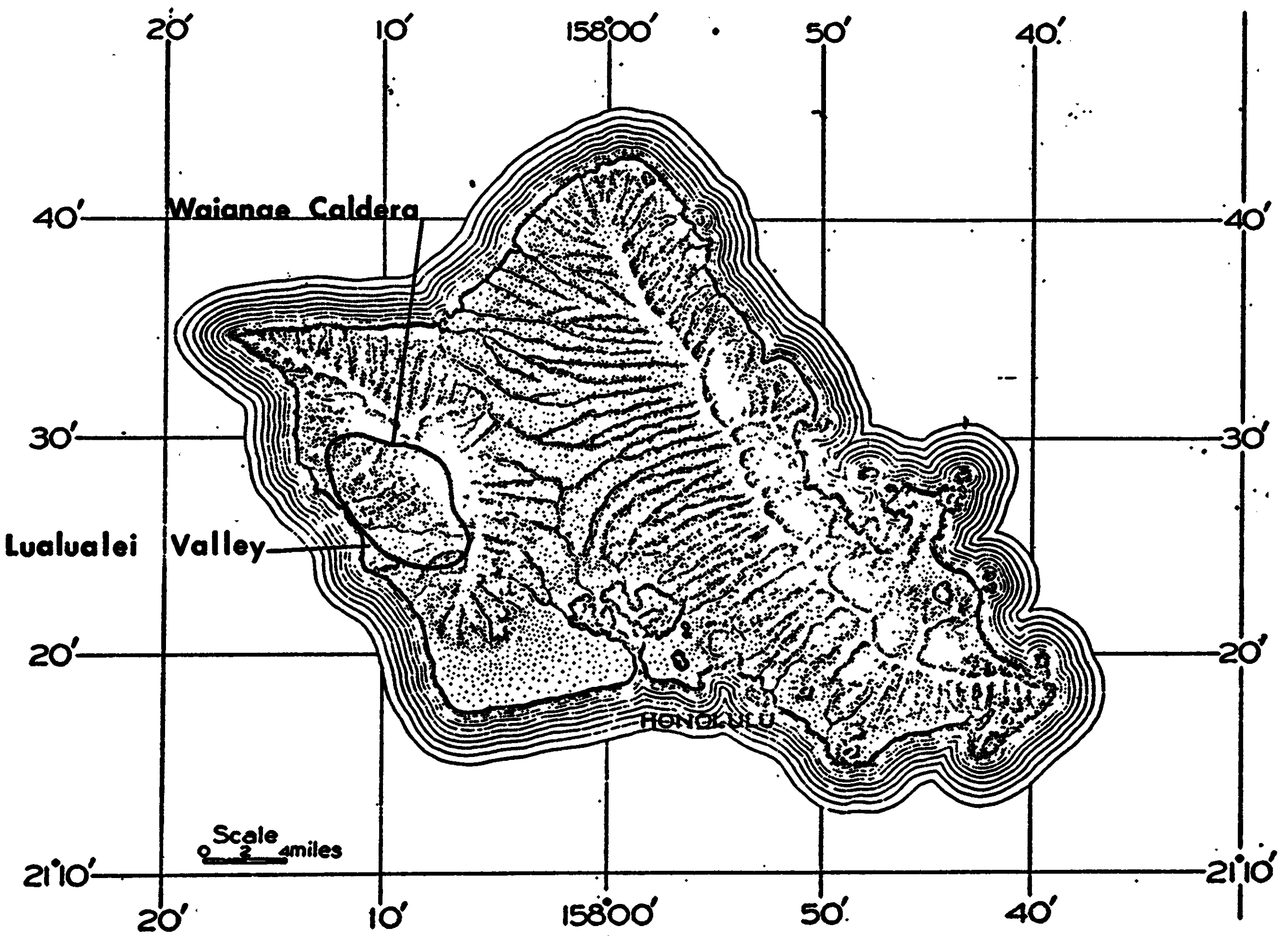

Figure 5. Shaded relief map of the island of Oahu, showing location of the Waianae Caldera (after Stearns, 1939)

There are no faults large enough to justify individual descriptions in or near the study area. Numerous dikes of different sizes suggests lateral displacement and jointing of the host rock with each injection. Puu Kailio, which is a hill located at the head of Lualualei Valley, was a place of intense volcanic activity; therefore, it was decided that the Kailio syncline was merely a sag in the flows produced by local withdrawal of support (Stearns, 1966). The anomaly is located about 2.5 miles south-southwest of this syncline (Fig. 2).

REVIEW OF PREVIOUS WORK

Gravity Studies

Detailed gravity surveys may be useful in many cases to explain the structural setting and locate anomalies of possible geothermal significance, provided the disturbing effects of nonrelevant structures in the area can be removed. The existence of various forms of hydrothermal alteration of reservoir rocks in geothermal areas is well known. Hochstein and Hunt (1970) have shown, by measurements on 77 samples, that there is a significant increase in density with increase in rank of hydrothermal alteration and that there is a density contrast of 0.3 to 0.4 g/cm^3 between hydrothermally altered and unaltered rocks of the same geological unit. Rex (1968) pointed out that it had been known for some time that an empirical correlation existed between high heat flow areas and gravity highs. Besides geothermal reservoirs, structures such as igneous intrusions, grabens, volcanic plugs and rift zones cause local gravity highs. Gravity lows are usually associated with sedimentary sections with considerable thicknesses.

In recent years, extensive gravity studies were made on the island of Oahu (Woollard, 1951; Woollard et al., 1964). The Bouguer gravity anomaly map of Oahu (Fig. 6) shows a positive anomaly of 115 mgal magnitude associated with the Waianae Caldera and a +50 mgal anomaly associated with the

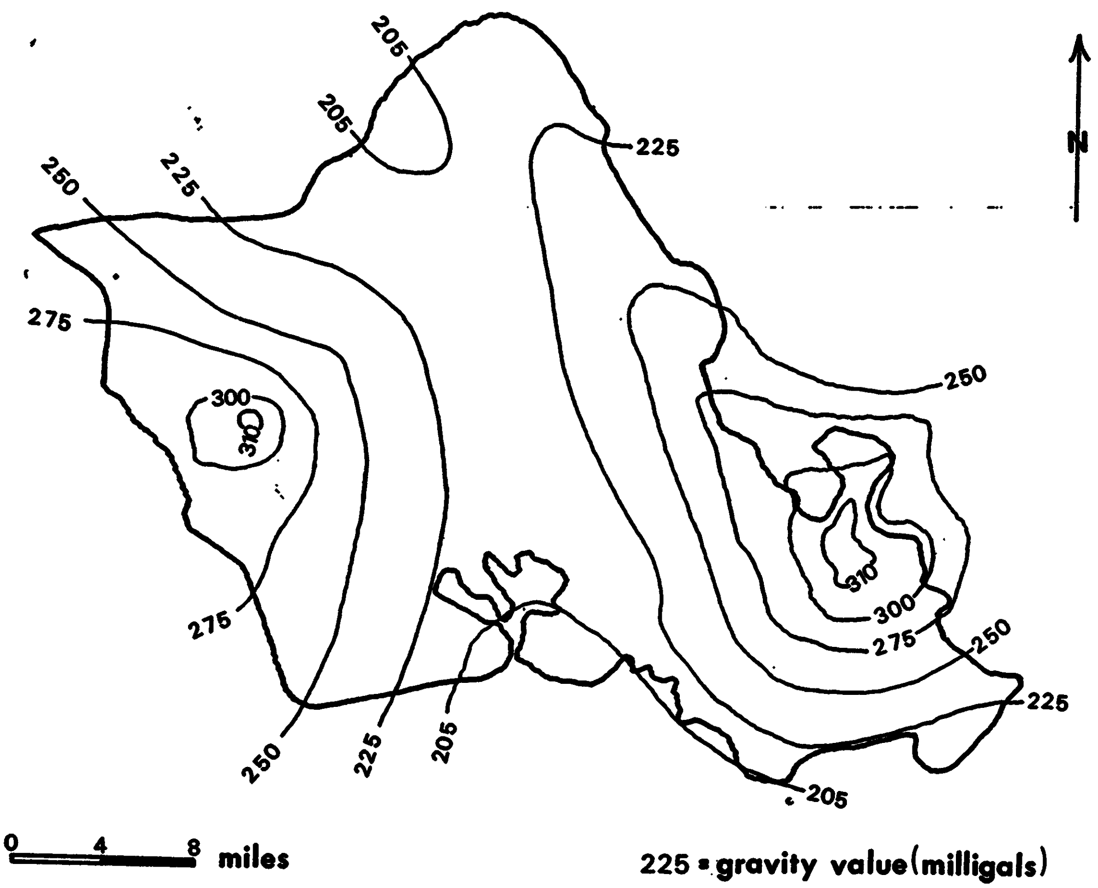

Figure 6. Bouguer gravity anomaly map of the island of Oahu
(after Strange, Machesky, and Woollard, 1965)

major rift zones. The gravity anomaly over the caldera was interpreted to be caused by a dense volcanic plug (3.2 g/cc) located at a shallow depth (about 800 m), extending to a depth of at least 5.5 km (MacDonald, 1965).

Both volcanic plugs with their high densities and geothermal systems cause high gravity values. If a geothermal system is located over a volcanic plug, the Bouguer gravity map of the area will show the additive effects of the plug and the system. The effect of the plug has to be removed in order to study the data to locate the system. This might not be easy to do, since the dimensions and the density distribution of the plug has to be determined accurately.

Aeromagnetic Study

Magnetic anomalies result from changes in the magnetic characteristics of rock masses which, in general, can be related to the percentage of magnetite and ilmenite present. Hydrothermal alteration of rocks may cause mineral changes which convert magnetic materials to non-magnetic and a geothermal area may be distinguished by a magnetic low. However, the majority of known areas of thermal activity are not marked by conspicuous lows, and magnetic patterns are often very complex, and many of the lows have no evident relation at all to present-day thermal activity (Banwell, 1970). The reasons may be:

1. A different distribution of hydrothermal systems over the area in the past.

2. Cancellation of the fields of several layers, caused by the reversals of the earth's field (Strangway, 1970).

A magnetic study of Oahu was made (Malahoff and Woollard, 1964). Aeromagnetic profiles flown at 10,000 feet were used to plot a total force magnetic map of the island (Fig. 7). Dipolar magnetic field effects measured over the Waianae Range were interpreted as representing vertical intrusive rocks intruded into the volcanic domes along elongate rift zones, because of their intensity and wavelength. The Waianae Caldera is marked by a 650-gamma, normally-polarized magnetic anomaly and the primary rift zones are marked by lenticular dipole anomalies (Fig. 8). The analysis of the magnetic field shows that the Waianae Volcanic Vent Zone is located at a depth of 800 m and extends to a depth of 5 km with an average width of 9 km (Malahoff and Woollard, 1964). The results of the aeromagnetic study correlate well with the results of the gravity studies.

The magnetic field associated with the Waianae Caldera and the primary rift zones dominates the magnetic field in the area. Therefore, a geothermal system located over the vent zone would not have a high enough magnetic effect to be noticeable with a study of such little detail.

Electrical and Seismic Study

A series of seismic refraction surveys were made over the Hawaiian arch, the trench and the ridge (Furumoto, et al, 1968). Variations in crustal thickness along the Hawaiian Archipelago and high seismic velocities approaching close to

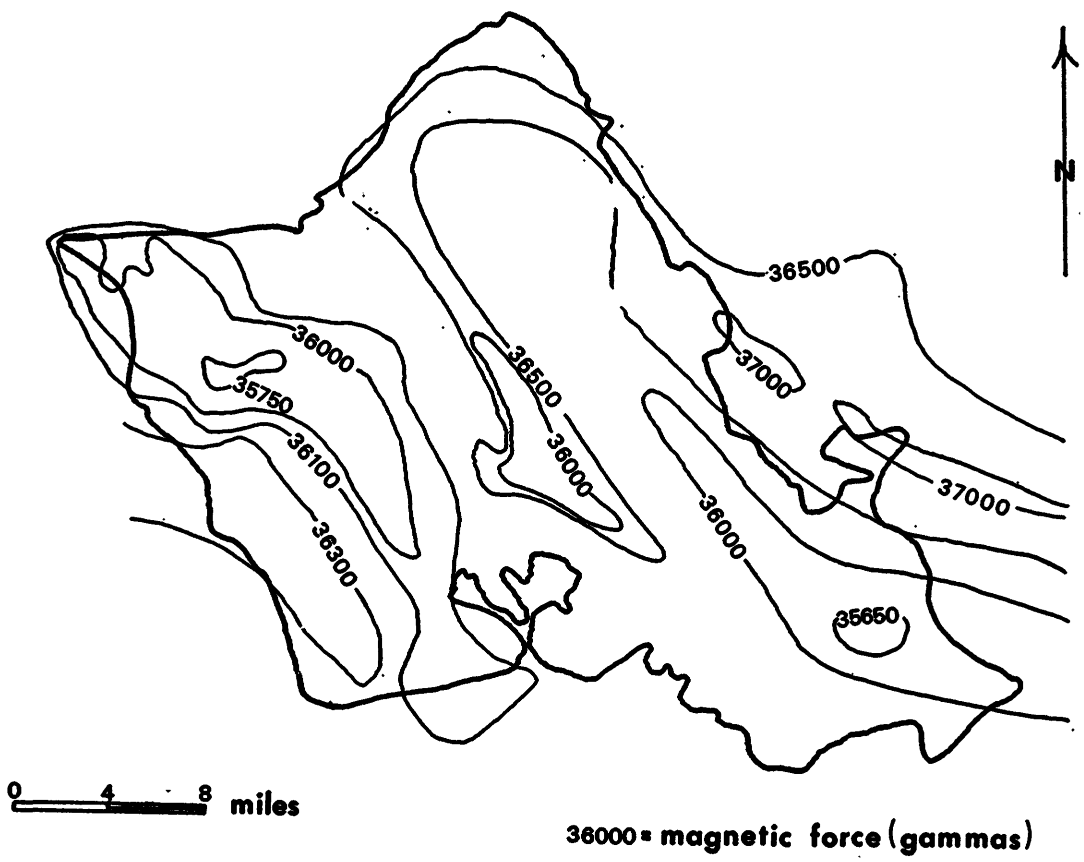

Figure 7. Total force magnetic map of the island of Oahu
(after Malahoff and Woollard, 1966)

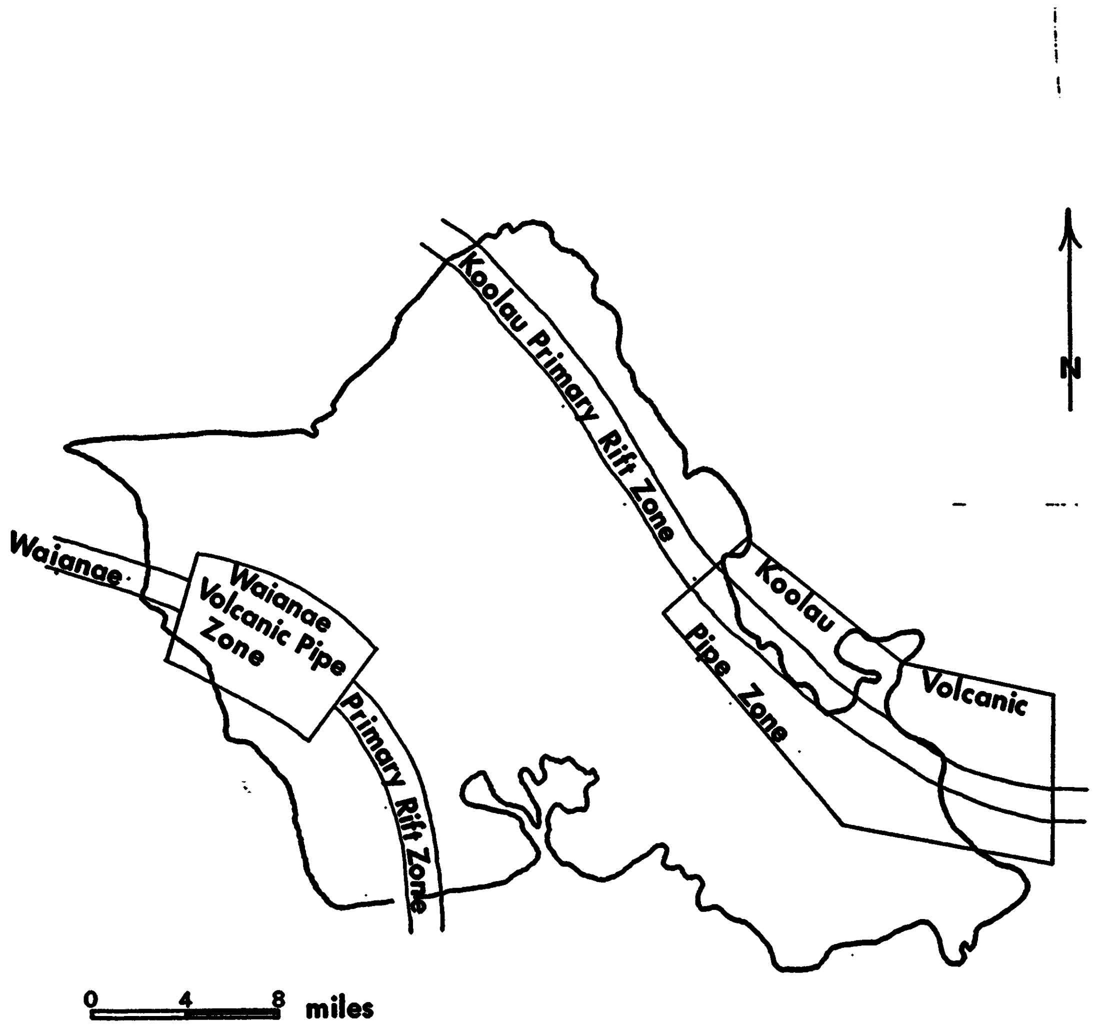

Figure 8. The primary rift zones and volcanic pipe zones of the island of Oahu (after Malahoff and Woollard, 1966)

the surface in the northwestern part of the ridge was found. Variations in crustal thickness were explained by differential subsidence of the islands to reach isostatic equilibrium. Seismic velocities greater than 7 km/sec beneath the Waianae Caldera as compared with 4.6 km/sec in surrounding material confirmed the presence of a dense volcanic plug as indicated by gravity and magnetic studies.

Intermediate and deep electrical soundings were made using the Schlumberger and the bipole-dipole equatorial electrode configurations near the town of Waialua on Oahu (Zohdy and Jackson, 1968). The purpose of the study was to determine the applicability of direct current resistivity methods for locating fresh water aquifers. The conclusions which will be helpful in explaining the resistivities associated with the Lualualei Naval Magazine are listed below:

1. A definite increase was observed in the clay resistivity away from the shoreline. This increase reflects primarily the decrease in salinity of the ground water that saturates the clay.

2. The resistivity of the Waianae basalt when saturated with saline water is exceptionally low (30 ohm-m) (Fig. 9).

3. The resistivity of fresh basalt saturated with fresh water, in general, is 300 to 700 ohm-m.

4. The Ghyben-Hertzberg relationship predicts that in coastal areas underlain by salt water the fresh-salt water interface will be depressed approximately 40 feet below sea level for every one foot rise of fresh water above sea level (Todd, 1959). (Under hydrodynamic conditions, Ghyben-Hertzberg ratio should be higher than 40:1.)(Zohdy and Jackson, 1968).

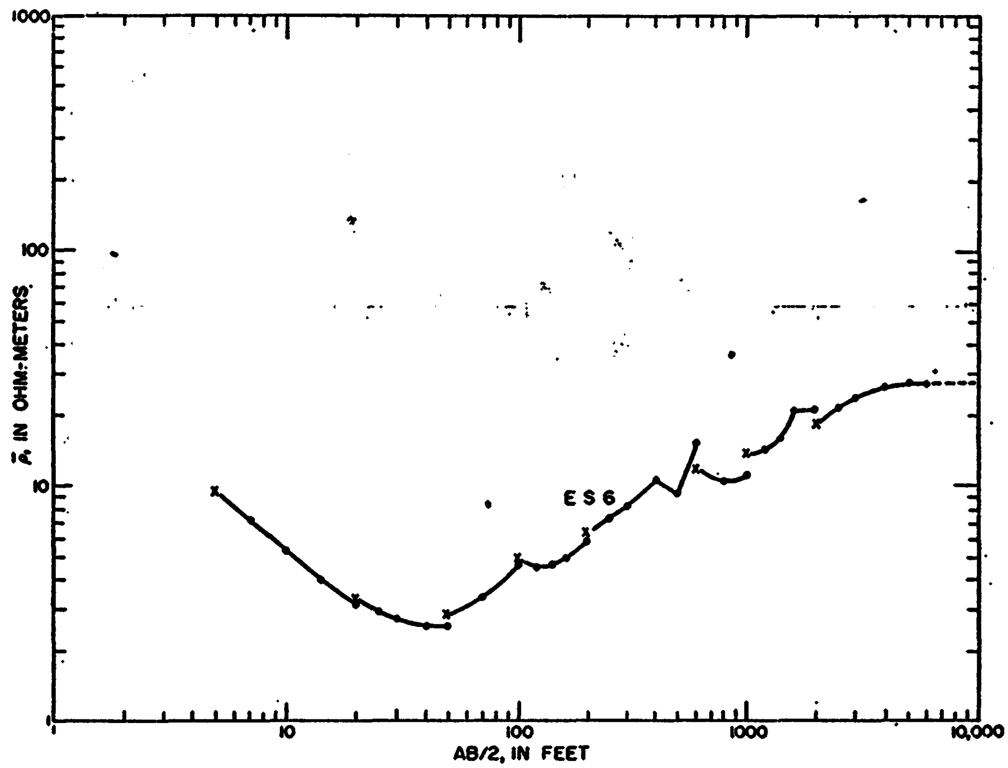

Figure 9. Schlumberger sounding curve over the Waianae basalt near Waialua (after Zohdy and Jackson, 1968).

SURVEY TECHNIQUES

Rotating-Quadripole Survey

Description of the Method: The rotating-quadripole technique is an electrical resistivity method which makes use of two dipole sources oriented at approximately right angles to each other. In fact, conventional dipole mapping procedures were used in the field (Furgerson, 1970, and Jordan, 1974); however, the data were treated differently (see Appendix II).

A suitable location was selected to set up a fixed d-c current source, keeping in mind the boundaries of the study area. Then, two holes 800 meters apart, were dug to bury two tin sheets, 3 feet by 4 feet. In order to reduce the contact resistance, salt and water were used. These two source electrodes were connected with #12 insulated, copper wire. To generate an electric field, a 2.5 kw generator was used. The 1-phase, 120v a-c, 60 hz output of the generator was passed through an asymmetrically-timed switching circuit and then rectified to d-c current. The asymmetric square-wave output of the rectifier was fed into the source wire. The relative polarity of the voltage drop along receiver wire was determined by observing the asymmetry of the square-wave output.

The field measurements were made a quarter of a mile apart from each other along the roads and near the ammunition magazines. At every station, two components (preferably orthogonal) of the earth potential were measured. To do this, two non-polarizing receiver electrodes were placed 30 meters apart and connected to a d-c amplifier with #12 insulated copper wire. The output of the amplifier was recorded with a potentiometric chart recorder. A Brunton Compass was used to determine azimuths of both components. Measurements were made at 103 stations around the first source. Then the second source was set up at a 96^{o} angle to the first source. Measurements were repeated occupying the same stations.

Two voltage components for each source were divided by the receiver length (30 m) to obtain electric field components and added vectorially to determine the total electric fields for both sources. If both sources were turned on, there would be only one total electric field and it can be obtained by orthogonal addition of the total electric fields of the two sources. The fields from the two sources can also be added with appropriate weights to rotate the total electric field 180^{o}. A set of apparent resistivities for every station was calculated using the rotating quadripole equation (see Appendix I for the equation, Appendix II for the computer program, and Appendix III for the data obtained in the field). Out of 40 resistivity values the best (the highest) value was selected for every station.

Interpretation of Field Data

Best Apparent Resistivity: The dipole mapping technique has been used extensively to determine lateral resistivity variations due to conductive bodies at depth, such as geothermal reservoirs. This fast d-c resistivity method also reveals information about the geologic structure of an area provided a resistive basement is present, and can be used for depth estimations. However, the technique is not problem free. The resistivity distributions from source #1 (Fig. 11) and from source #2 (Fig. 14) are not the same. If a third dipole source were put in the area, the result would probably be a third different resistivity distribution. It is concluded from the discussion above that a single dipole source is not adequate to determine the best resistivities. Being located of the end or the center of the dipole also has an effect on the resistivities of an area. An area located of the end of the dipole has lower resistivities than the same area if it should be located of the center of the source (Figs. 11 and 14). This is caused by the behavior of the current flow of the end of the dipole. Still another problem is false values caused by lateral inhomogeneities. Presence of a fault-like boundary between a region with moderate resistivities and another region with high resistivities will cause "false" anomalies to be observed at specific locations along the fault-like boundary (Fig. 10) (Grose and Keller, 1974).

To eliminate the observed false anomalies and to obtain resistivities as close as possible to the true resistivities multiple coverage must be provided. This can be done by randomly located multiple sources or by the rotating-quadripole method. In the rotating quadripole method, two dipole sources at right angles to each other are used (see Appendix II).

Figure 11 shows the apparent resistivity distribution due to source #1. The 75 ohm-m contours indicate the presence

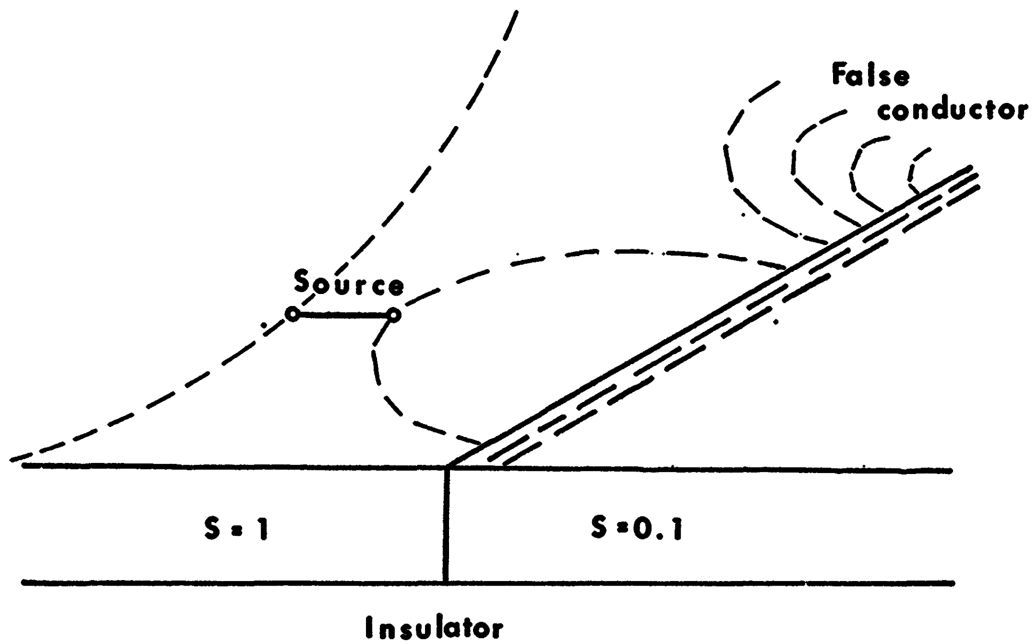

Figure 10. Observed false conductor along the fault like boundary (after Grose and Keller, 1974)

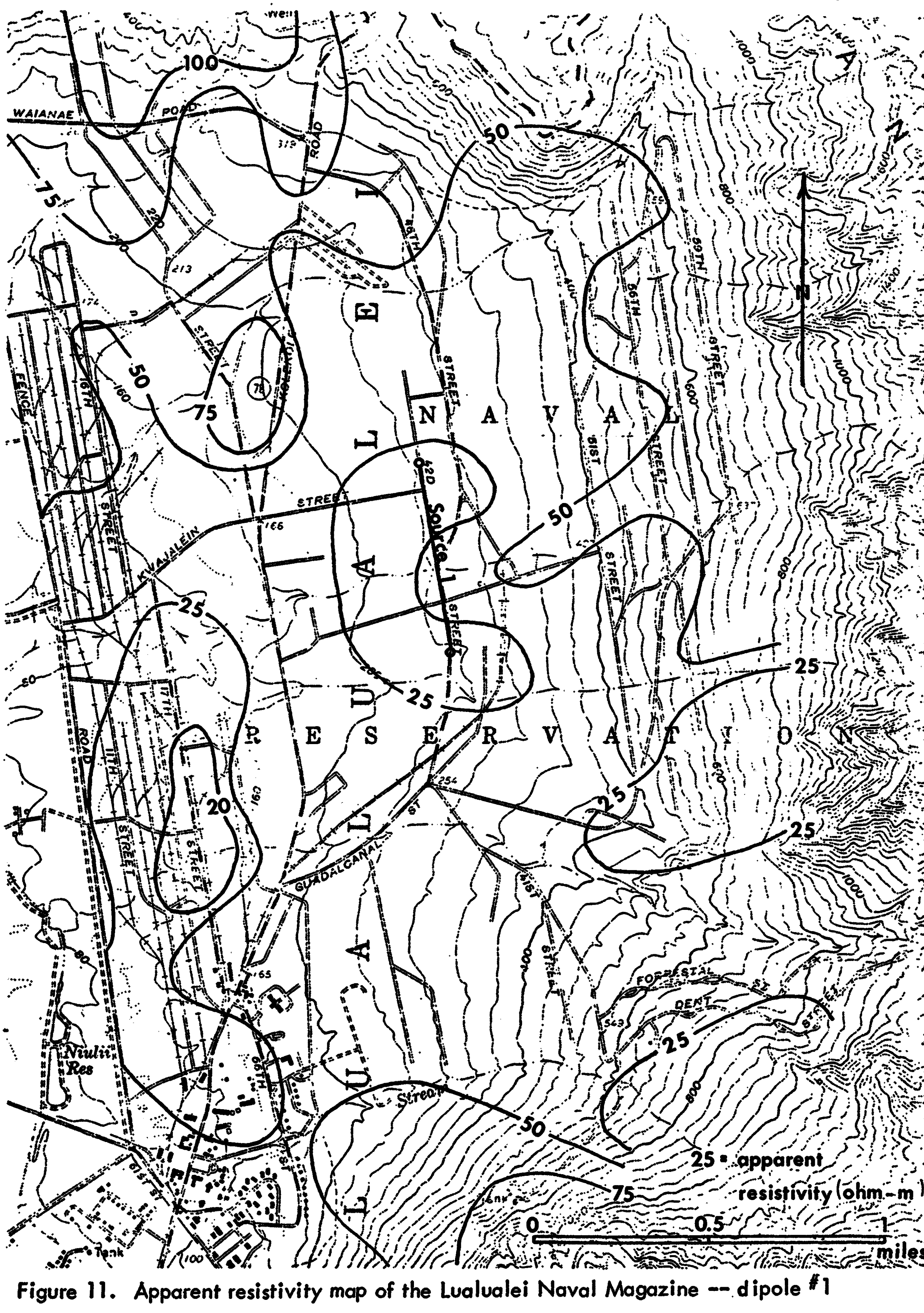

Figure 11. Apparent resistivity map of the Lualualei Naval Magazine -- dipole #1

of a resistive basement (the volcanic plug). If it were possible to take measurements farther east and west, the 75 ohm-m contours would have probably closed to the east and the west. The presence of a closed 25 ohm-m contour around the source indicates a thin conductive surface layer. The 25 ohm-m contour located to the southwest of the source is considered anomalous because of its closure and relatively lower resistivity. The low resistivities could be caused by a geothermal system, either modern or ancient, or they could be the result of thickening of the alluvial deposits in that area.

A histogram of the resistivity distribution observed from source #1 deviates from a normal distribution between 20 and 32 ohm-m (Fig. 12). These anomalous values were measured mainly in and around the area with low resistivities to the southwest.

A scatter diagram was constructed by plotting the resistivity values against the distance to the nearest source electrode (depth of current penetration) (Fig. 13). Absence of a recognizable pattern (clustering of points on a 45° angle with increasing distance from the source) indicates that lateral changes in resistivity obscure any effect of layering in the rocks of the area. However, increase in resistivities after a distance of 1 km suggests the presence of layering.

The apparent resistivity map from source #2 (Fig. 14), in general, has the same pattern as the first source. The 75 ohm-m contours are closer to each other than the 75 ohm-m contours for the first source. This is caused by the orientation of the dipole sources. The resistivities to the north

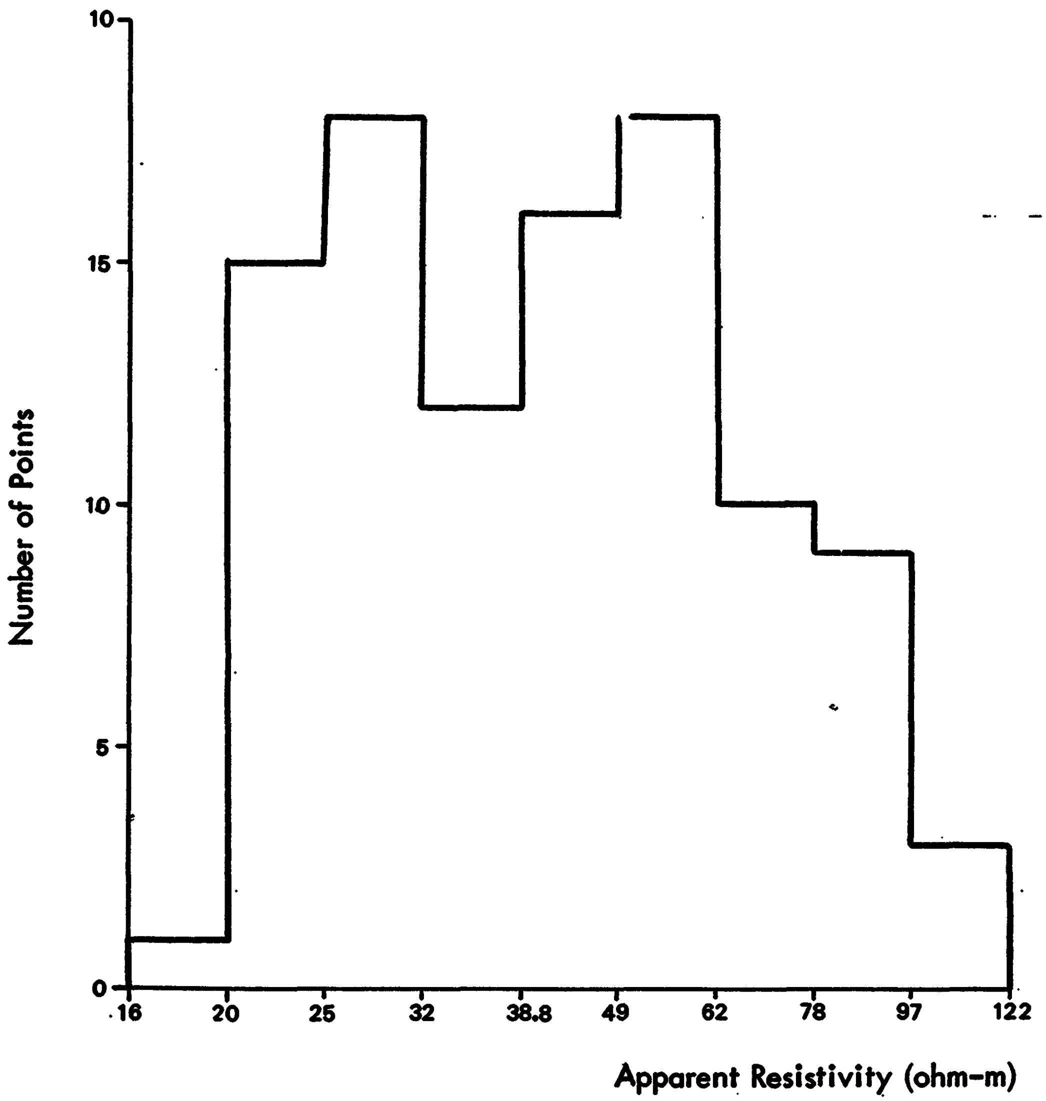

Figure 12. Distribution of apparent resistivity -- dipole #1

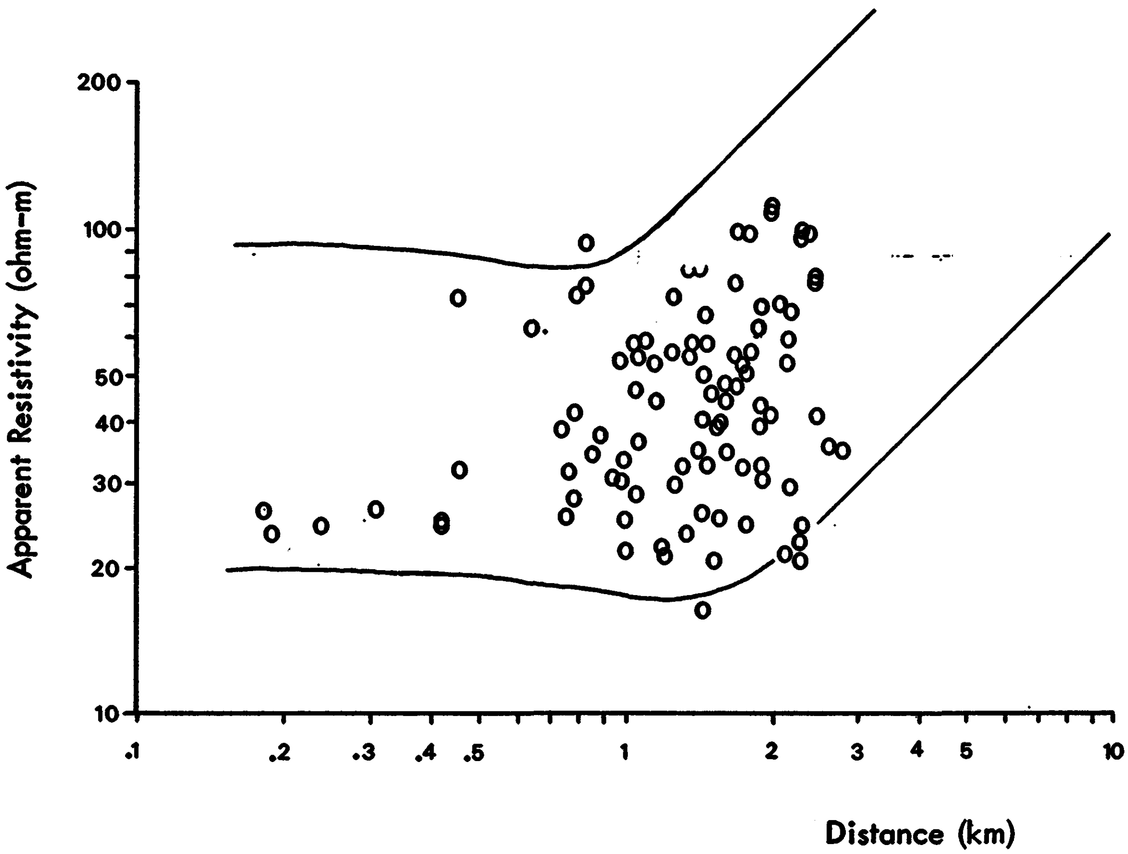

Figure 13. Apparent resistivity scatter diagram -- dipole #1

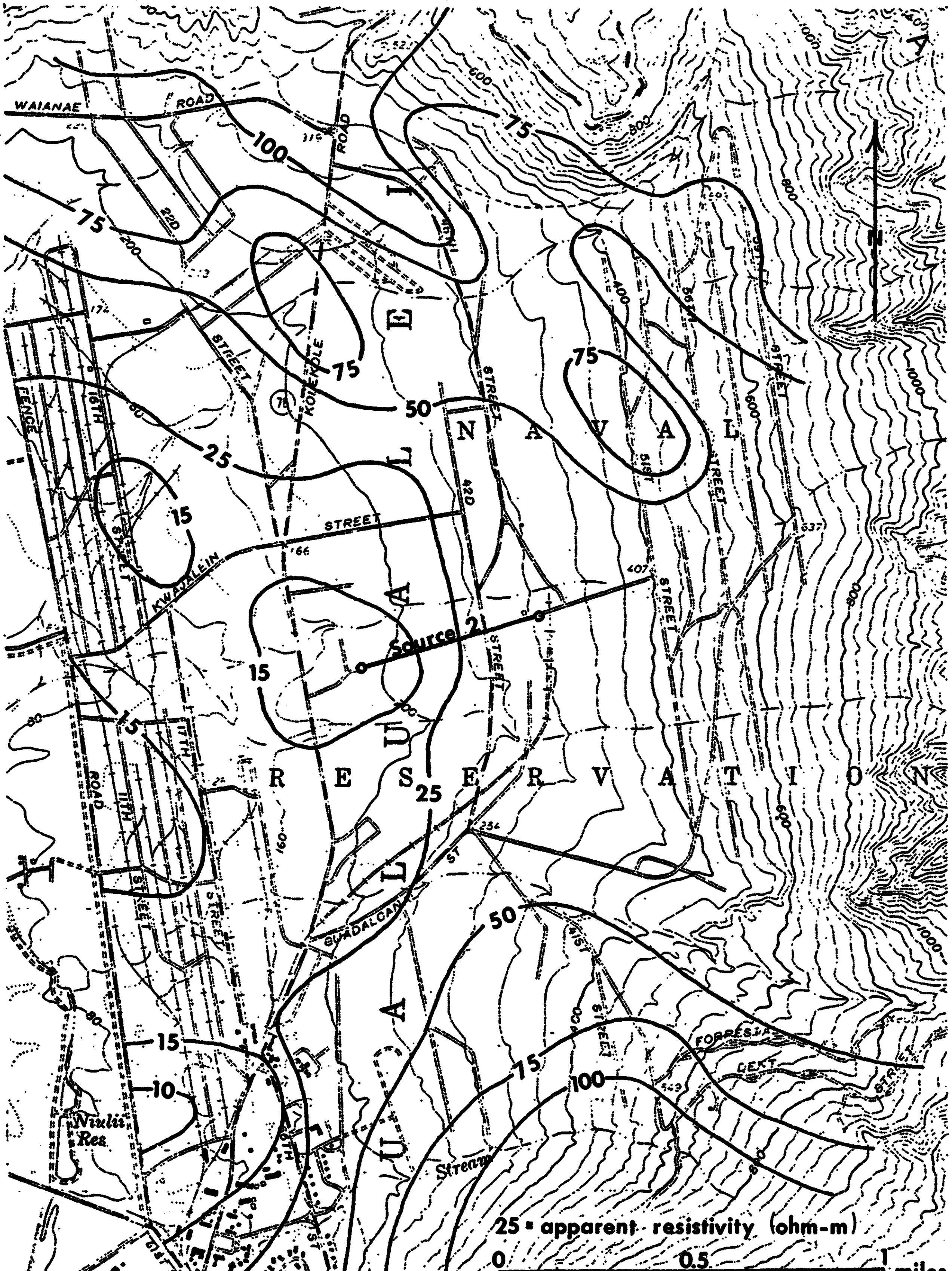

Figure 14. Apparent resistivity map of the Lualualei Naval Magazine -- dipole #2

and south of source #2 are, in general, higher than the resistivities from source #1 in the same areas. However, to the east and west, they tend to be lower. Presence of resistivities less than 15 ohm-m to the southwest of the source indicates the presence of a conductive body in that area. The open contours would probably close if more data were available to the west of the Fence Road. It is believed that the open contours are partly due to the thickening of the alluvial layer to the west and because this area is oriented off the end of the source, the current does not feel the effect of basement as near to the source as it does for the area of the center of the source (Jordan, 1974).

The histogram which shows the resistivity distribution for source #2 (Fig. 15) has an anomalous distribution between 9 and 42 ohm-m. These resistivity values are located to the west and the southwest of the source.

A scatter diagram with resistivity values plotted against distance from the nearest source electrode (Fig. 16) indicates the absence of an observable effect of layering in the area. However, layering in the area could be suggested, because the points tend to rise along a 45° angle after a distance of 0.6 km.

Despite the variations in resistivities obtained from sources #1 and #2, the results correlate fairly well. The data from these two sources were analyzed using the rotating-quadripole method.

Out of 40 resistivity values obtained by rotating the total electric field, the highest value was picked for every station (see Appendix II). These values are believed to be

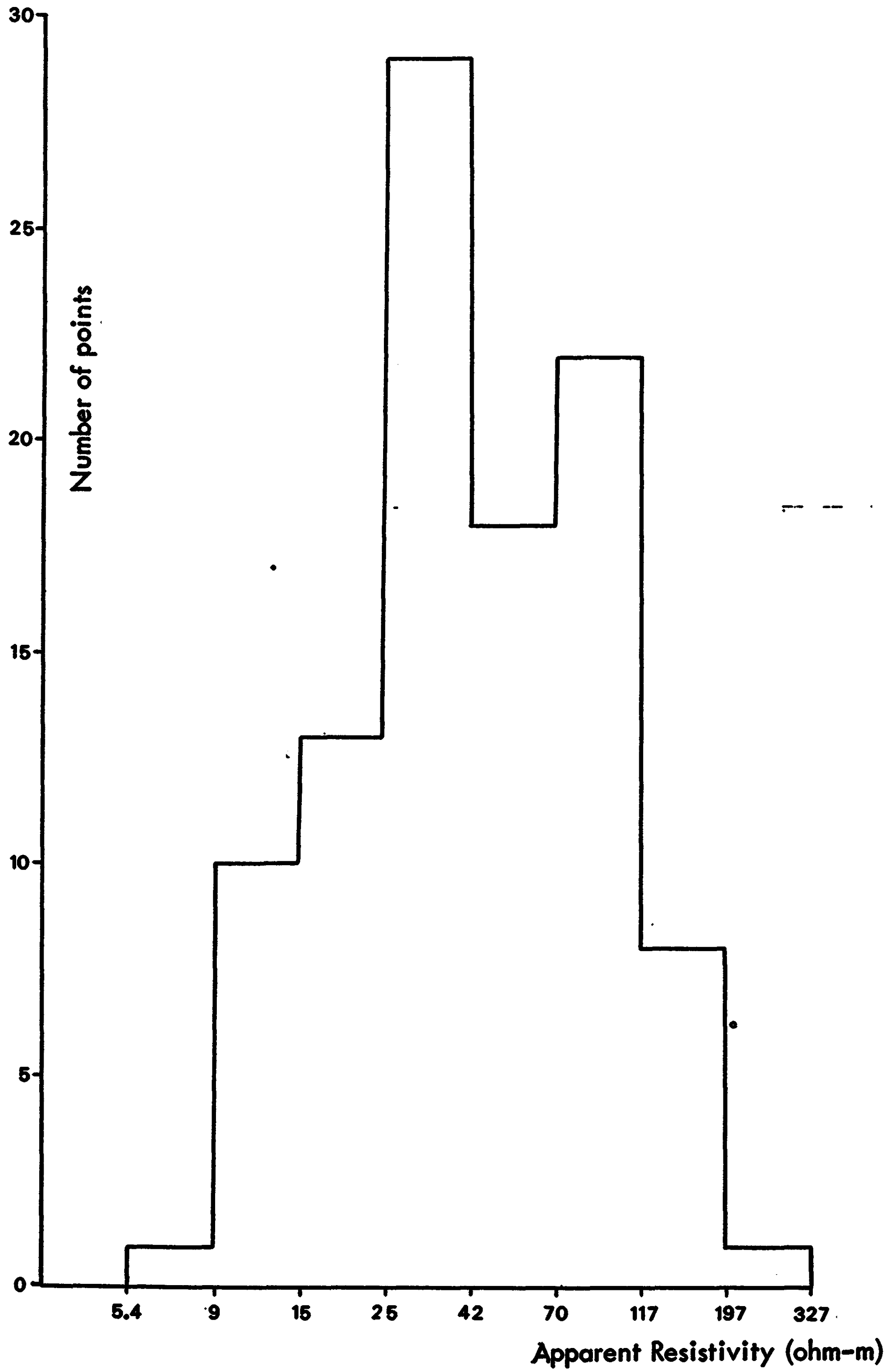

Figure 15. Distribution of apparent resistivity -- dipole #2

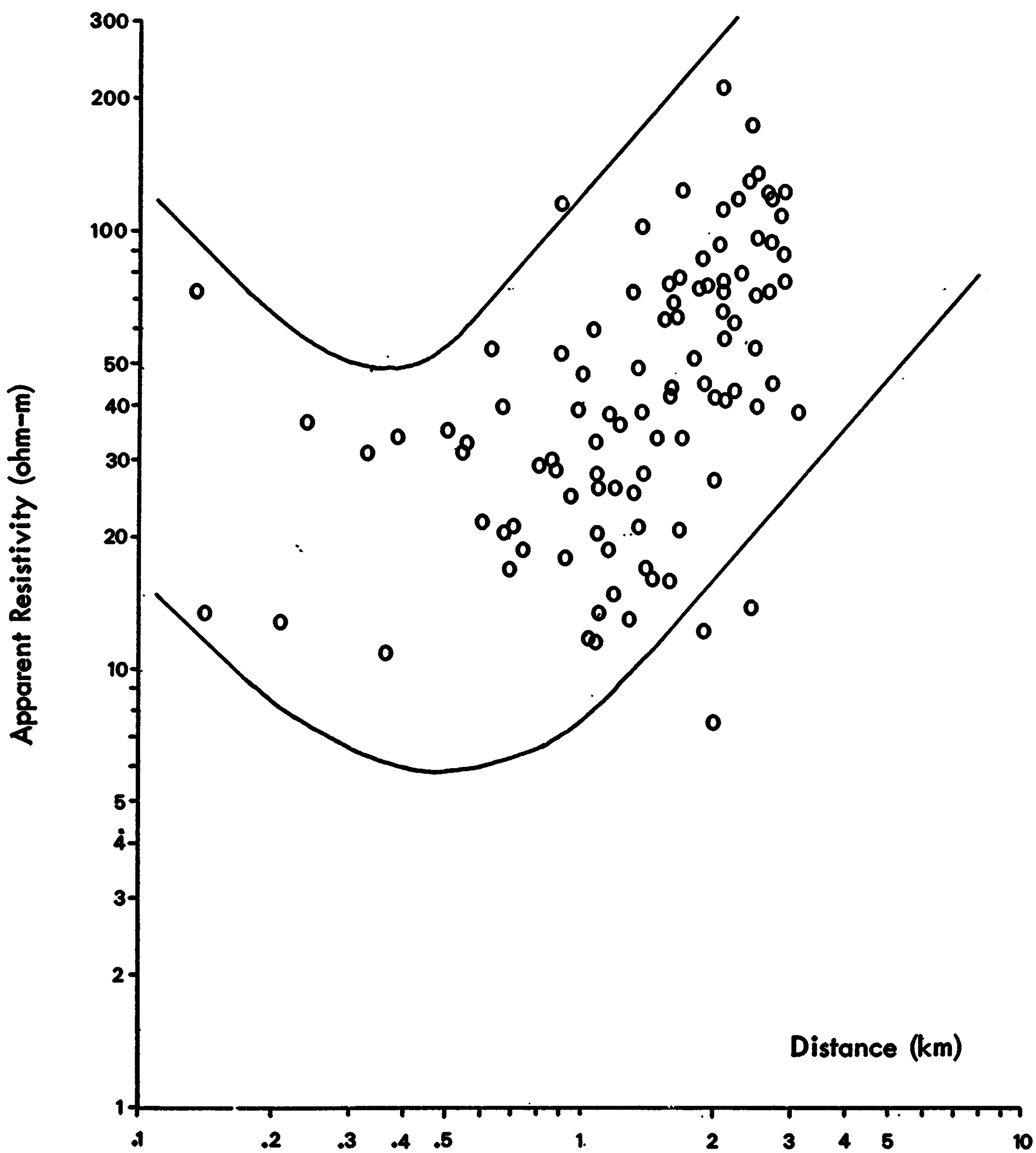

Figure 16. Apparent resistivity scatter diagram -- dipole #2

the closest to the true resistivities; therefore, they were called the best apparent resistivities. In almost all cases the best resistivities are higher than the resistivities obtained from the original dipole source.

Figure 17 shows the best apparent resistivity map of the study area. The 75 ohm-m contours and high resistivities indicate the presence of a resistive basement at depth. The resistive basement is believed to be the volcanic plug of the Waianae Volcano. A closed 35 ohm-m contour near the sources indicates the presence of a thin conductive surface layer. The 35 and 30 ohm-m contours to the southwest of the sources might be caused by a conductive body at depth.

A histogram showing the distribution of best resistivity values is presented in Figure 18. A deviation from a normal distribution occurs between 28 and 41.4 ohm-m, and these anomalous values were measured mainly in the conductive zone located to the southwest of the two sources (Magazines 11 and 12).

To construct a scatter diagram, best resistivities were plotted against the distance to the nearest of the four source electrodes. This distance is thought to be the depth of current penetration. The resulting scatter diagram (Fig. 19) suggests the presence of layering in the area, because the points tend to cluster along a 45° angle after 1 km distance.

Measure of Anisotropy: Conductive and resistive masses of rock change the direction of the current flow and amplitude of the electric field around them. If two dipole sources

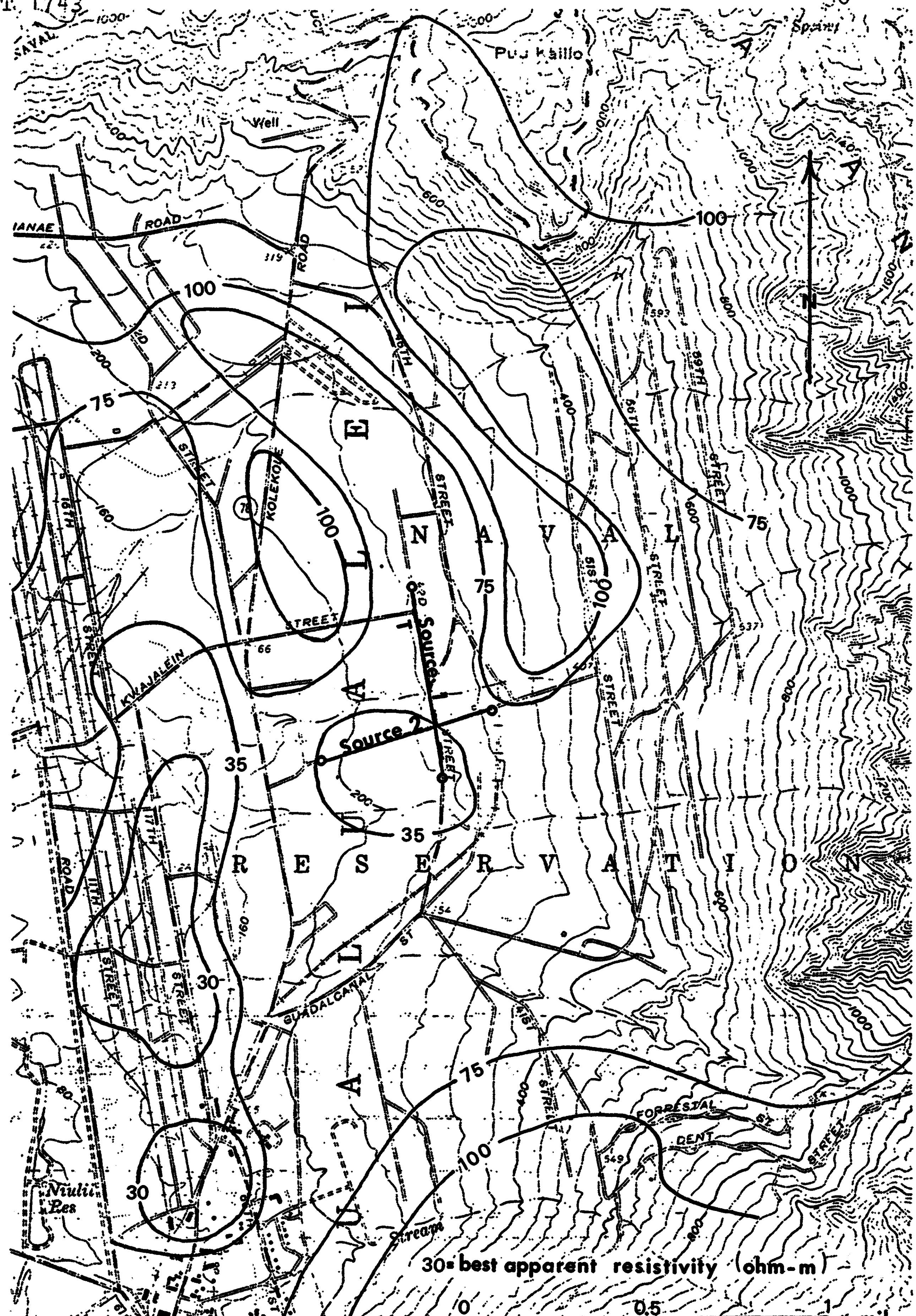

Figure 17. Best apparent resistivity map of the Lualualei Naval Magazine -- rotating-quadripole array

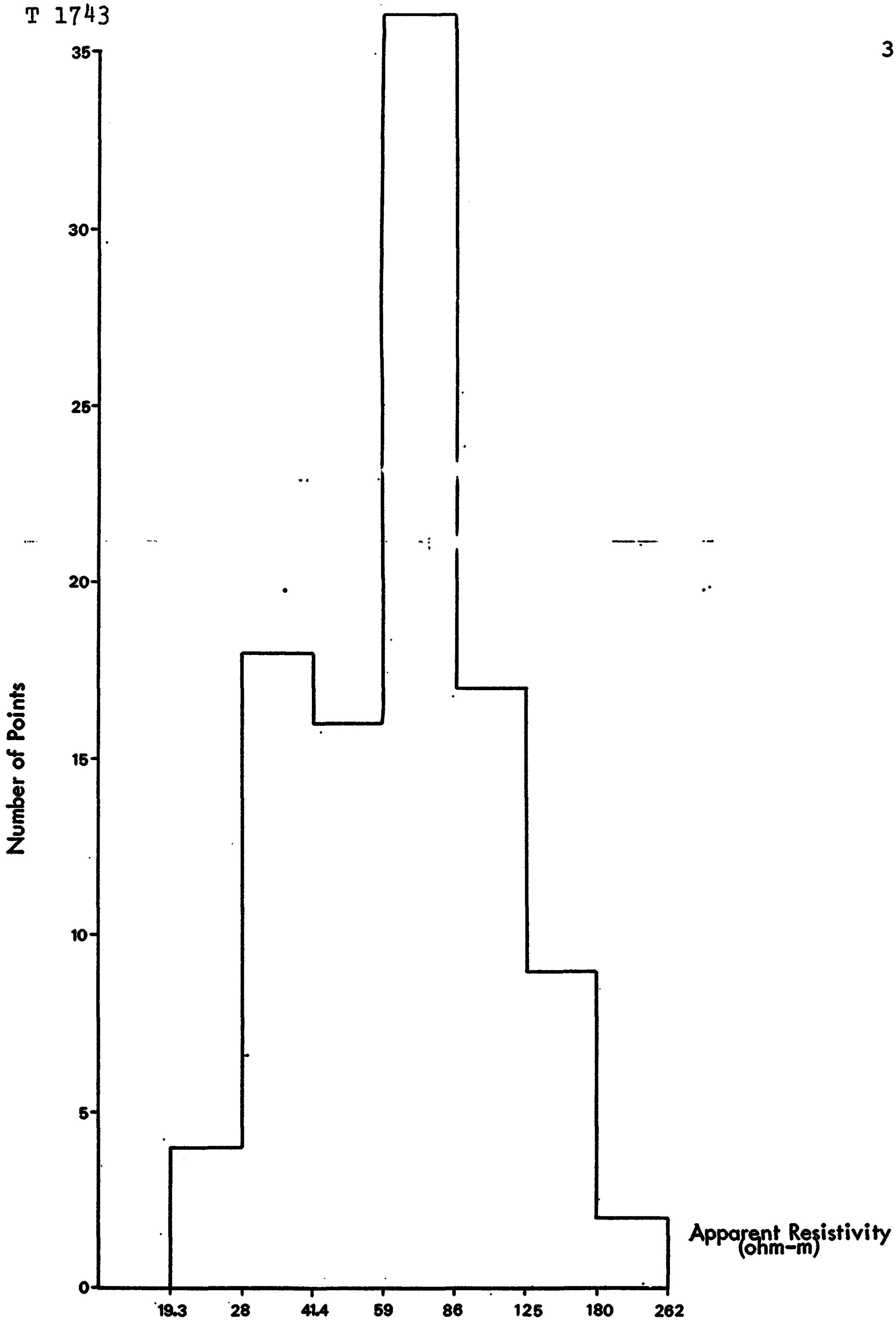

Figure 18. Distribution of best apparent resistivity -- rotating-quadripole array

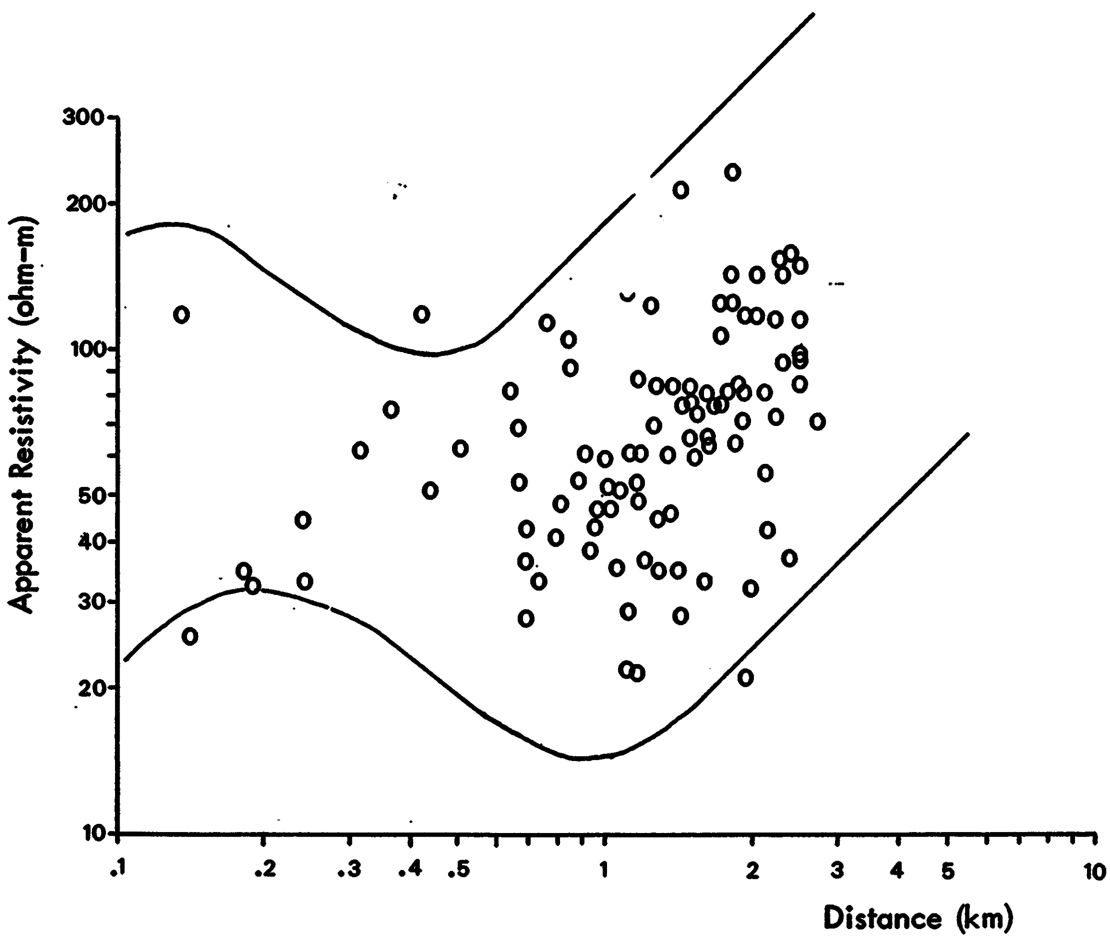

Figure 19. Best apparent resistivity scatter diagram -- rotating-quadripole array

at an angle to each other were set up near such a mass of rock, the directions of the current flows due to both sources would be affected to some degree. Depending on the conductivity or the resistivity of the body the angle between the two total electric fields would be changed. Depending on the angle between the two fields, low and high resistivities would result from the rotating-quadripole study of the data (Fig. 20 and Appendix II). The closer the angle between the two fields to 0° or 180°, the higher the ratio of maximum resistivity to minimum resistivity (Fig. 21 and Fig. 22).

Out of forty resistivity values for every station, maximum and minimum values were picked. The ratios of maximum to minimum values were determined. These ratios will be called anisotropy ratios since they are a measure of anisotropy. Figure 23 shows a contour map of the anisotropy ratios for the area. A high value (5) surrounds the area to the north, the east, and the south indicating the presence of an anisotropic medium at depth. A resistive volcanic plug is believed to be the cause of these high values. Very high anisotropic ratios were expected around the conductive zone to the southwest of the dipoles. However, the expected values were found only to the north and the northeast of the anomaly, and moderate values (3) to the east and south. An abrupt resistivity change occurs to the north and the northeast of the conductive zone; however, a gradual resistivity change takes place to the east (Fig. 17). Presence of a resistive zone near the

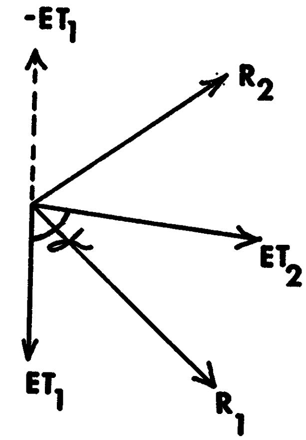

$\alpha > \beta \Longrightarrow R_{2\beta} < R_{2\alpha}$ and

$R_{1\beta} > R_{1\alpha}$

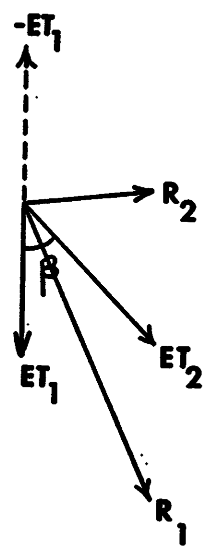

Figure 20. Orthogonal addition of two vectors and the effect of the angle between them on the resultant vectors

```
STATION NUMBER  23 AT A DISTANCE OF  Ø.86Ø KILOMETERS
TOTAL FIELD 1 IS  Ø.276E+Ø2 MICROVOLTS AT A BEARING OF 358. DEGREES
TOTAL FIELD 2 IS  Ø.421E+Ø2 MICROVOLTS AT A BEARING OF 1Ø6. DEGREES
```

E FIELD BEARING	TOTAL E FIELD	RESISTIVITY, OHM-METERS	
178.	27.62	3Ø.55	**Source 1**
173.	26.97	3Ø.24	
169.	26.48	3Ø.Ø3	
164.	26.15	29.95	**Minimum Resistivity**
16Ø.	25.99	3Ø.ØØ	
155.	26.Ø1	3Ø.19	
15Ø.	26.2Ø	3Ø.52	
146.	26.56	3Ø.98	
141.	27.Ø8	31.56	
137.	27.76	32.24	
133.	28.57	33.Ø2	
129.	29.52	33.86	
126.	3Ø.59	34.76	
123.	31.77	35.68	
12Ø.	33.Ø4	36.63	
117.	34.39	37.57	
114.	35.82	38.5Ø	
112.	37.32	39.41	
11Ø.	38.88	4Ø.29	
1Ø8.	4Ø.49	41.14	
1Ø6.	42.14	41.94	**Source 2**
1Ø4.	39.62	42.79	
1Ø2.	37.15	43.77	
99.	34.75	44.91	
97.	32.41	46.23	
93.	3Ø.17	47.73	
9Ø.	28.Ø4	49.37	
85.	26.Ø4	51.Ø3	
8Ø.	24.22	52.43	
74.	22.62	53.12	**Maximum Resistivity**
68.	21.28	52.51	
6Ø.	2Ø.25	5Ø.31	
52.	19.6Ø	46.85	
44.	19.35	42.96	
36.	19.51	39.37	
28.	2Ø.Ø9	36.47	
2Ø.	21.Ø4	34.31	
13.	22.32	32.77	
7.	23.88	31.72	
2.	25.66	31.Ø1	
358.	27.62	3Ø.55	**Source 1**

Figure 21. The set of values calculated for station 23 with the rotating-quadripole program

STATION NUMBER 102 AT A DISTANCE OF 1.774 KILOMETERS
TOTAL FIELD 1 IS [illegible].978E+21 MICROVOLTS AT A BEARING OF 65. DEGREES
TOTAL FIELD 2 IS 0.242E+21 MICROVOLTS AT A BEARING OF 61. DEGREES

E FIELD BEARING	TOTAL E FIELD	RESISTIVITY, OHM-METERS	
245.	9.78	55.64	**Source 1**
245.	9.17	54.61	
245.	8.56	53.37	
245.	7.95	51.87	
245.	7.34	50.07	
246.	6.74	47.93	
246.	6.13	45.40	
246.	5.52	42.44	
246.	4.91	39.01	
246.	[illegible]	35.12	
247.	3.69	30.78	
247.	3.08	26.04	
248.	2.47	21.01	
249.	1.86	15.78	
251.	1.25	10.52	
258.	0.65	5.37	
325.	0.15	1.23	**Minimum Resistivity**
53.	0.60	4.70	
57.	1.20	9.04	
60.	1.81	13.06	
61.	2.42	16.73	**Source 2**
61.	2.79	20.38	
62.	3.15	24.36	
63.	3.52	28.65	
63.	3.89	33.18	
63.	4.26	37.84	
64.	4.63	42.46	
64.	4.99	46.84	
64.	5.36	50.79	
64.	5.73	54.11	
64.	6.10	56.69	
64.	6.47	58.51	
65.	6.84	59.62	
65.	7.20	60.11	
65.	7.57	60.12	**Maximum Resistivity**
65.	7.94	59.76	
65.	8.31	59.15	
65.	8.68	58.37	
65.	9.05	57.50	
65.	9.42	56.58	
65.	9.78	55.64	**Source 1**

Figure 22. The set of values calculated for station 102 with the rotating-quadripole program

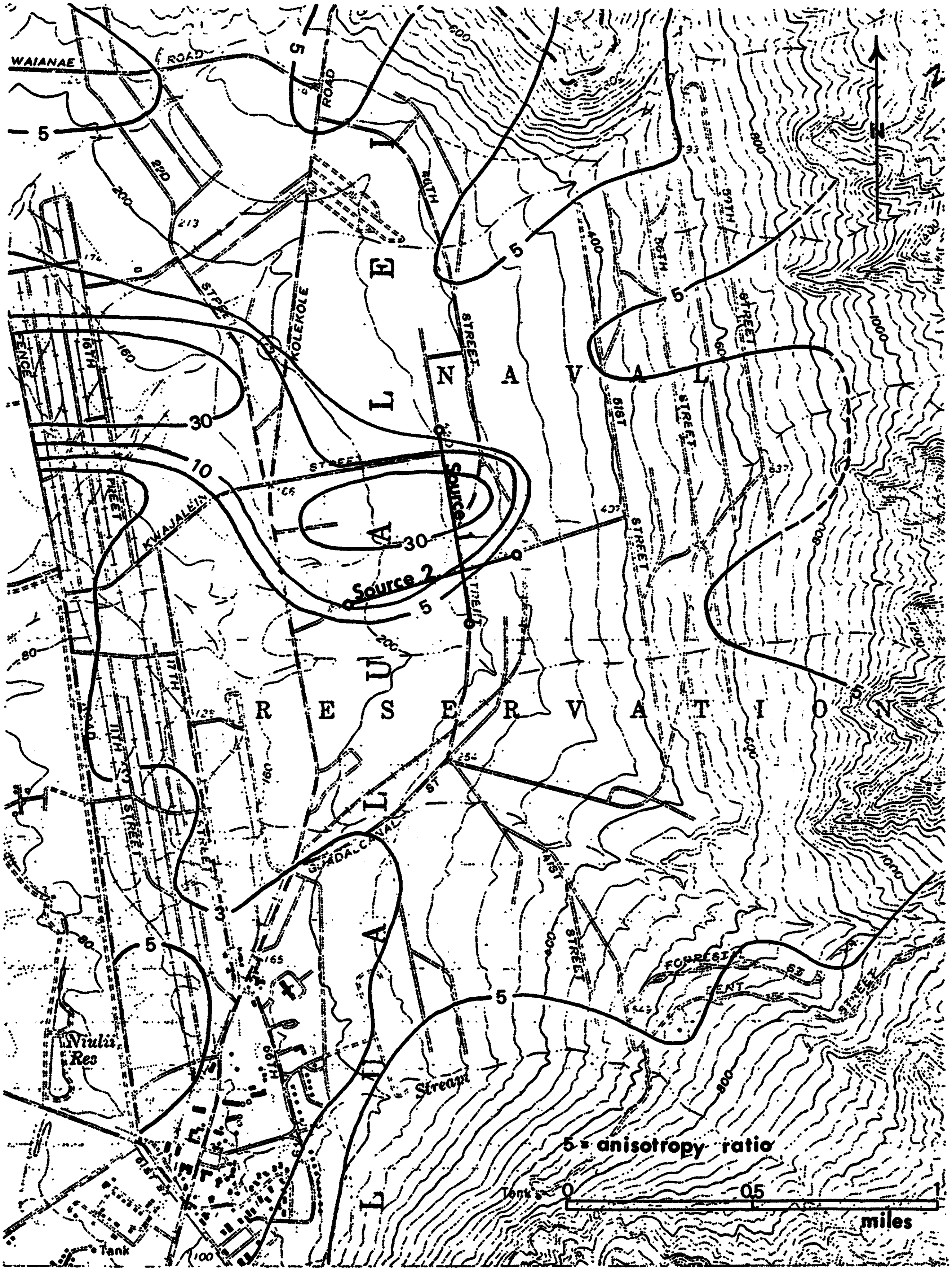

Figure 23. Anisotropy ratio map of the Lualualei Naval Magazine

conductive zone has an additive effect on distorting the direction of the current flow in the area. Thus, the angle between the two directions are reduced and the anisotropy ratio is increased. A monotonous resistivity distribution to the east of the anomaly is believed to be the reason for the moderate anisotropy ratios in that area.

Temperature Survey

Geothermal exploration should not be limited to the vicinity of areas of heat escape in the form of geysers, fumaroles, sulfatras and hot springs. A reservoir of moderate size with an upper surface at 2 km depth would approximately double the normal geothermal gradient over an area of a few square kilometers (Banwell, 1970). Therefore, detection of a sealed reservoir with no convection to the surface is not difficult. Surface temperature and heat flow measurements at 1 to 2 m depths have been successful in mapping high temperature zones and in evaluating the hot water distribution below the surface (Yuhara, 1970 and Kromar et al, 1970). These observations provide a rapid and direct way of making an estimate of the size and energy potential of a system. When making or interpreting a shallow temperature survey, hydrological conditions in the area including rate and direction of ground water movement have to be considered. Because movement of ground water can carry away the conductive heat flow from a thermal anomaly, it can displace the surface temperature patterns. Instrumental errors may result from using thermistor probes for temperature measurements; the overall error has been estimated to be between 0.01 and 0.05°C for measurements at a depth of 2 m (Dedkova, et al, 1970). Seasonal and weather changes and variations in surface cover are believed to have random effects on shallow temperatures.

Description of the Method: A shallow (1 meter deep) temperature study was carried out in the Lualualei Naval Magazine in order to determine the shallow temperature distribution and locate areas with anomalous temperature gradients. A simple mechanical device called a dongeyknocker made of mild steel was used to punch holes in the ground (Fig. 24). A YSI precision thermistor teflon probe was placed at the bottoms of these holes using a wooden rod. The resistance of the probe was measured with a digital multimeter. These resistances were converted to temperatures (°C) using a conversion table (see Table 2). The measurements were spaced closely (800 feet apart) over the resistivity anomaly to provide detail in that area. A wider spacing of 2000 feet was used for the measurements over the resistive zone. A total of 70 measurements was made including 7 to the west of the Fence Road where there is no resistivity information.

Interpretation of the Field Data

Ground Temperature: Measured temperature values represent ground temperatures and Figure 25 shows the ground temperature (at 1 meter depth) pattern of the area. Before

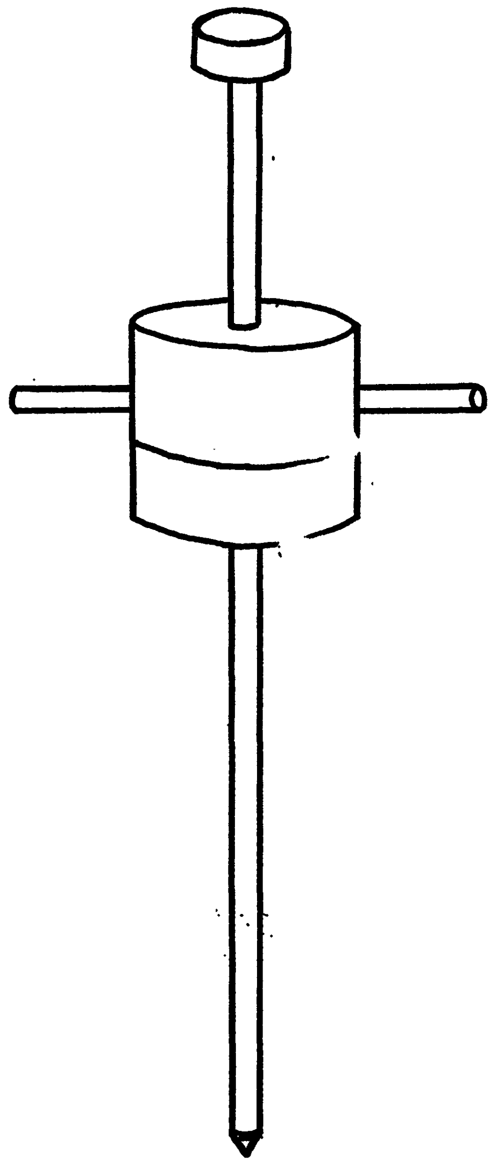

Figure 24. Dongeyknocker.

making an attempt to interpret the data, some important factors should be considered. Surface cover in the area is alluvium and major variations likely to cause false anomalies are unlikely. Since there is a difference of 2°C in temperatures between the cold and the warm zones, instrumental errors (.05°C or less) could not have changed the temperatures enough to distort the temperature pattern. Where ground water is confined between dikes, it is under static conditions. This is true for the basalts with numerous dikes below the alluvial fill; however, the alluvial section itself is believed to contain water under dynamic conditions.

It was discovered that the area with anomalous resistivities (less than 30 ohm-m) had, in general, a temperature of 26.3°C. Since the resistive zones had lower ground temperatures (as low as 24.3°C), it was concluded that the low resistivities to the southwest of the dipoles were caused by high temperatures at depth, possibly a sealed geothermal reservoir. The other temperature anomalies in the area (areas with temperatures higher than 26°C) are believed to be surficial features caused either by variations in the

Table 2. Resistance versus temperature for YSI precision thermistor teflon probe

Temperature (°C)	Resistance (ohms)
23	1076
24	1037
25	1000
26	963.4
27	928.9
28	895.9
29	864.1
30	833.7

surface cover or by the movement of the ground water in alluvium or both, and they are not supported by low resistivities except where there is no resistivity information.

Self-Potential Survey

Geothermal reservoirs contain ground water of differing temperature and chemical composition. Thermal gradients in pore water electrolytes and contact potentials between bodies of ground water of differing temperature and chemical composition may give rise to measurable electrical anomalies. In the course of resistivity surveys of thermal areas, high natural electrical potentials have been commonly observed (Banwell, 1970). These natural potentials may form a diagnostic pattern over the area. Such a survey would be valuable since it would have some depth penetration and point by point observations would be possible with small electrode spacings.

Description of the Method: A self-potential survey was carried out in order to determine if the area with low resistivities and high temperatures had anomalous self potentials. The measurements were made with a digital voltmeter using two non-polarizing electrodes with an electrode spacing of 200 m. A starting point with an assigned potential of zero was picked in an area with high resistivities (Fig. 26). Potential drops were measured along a continuous line, across

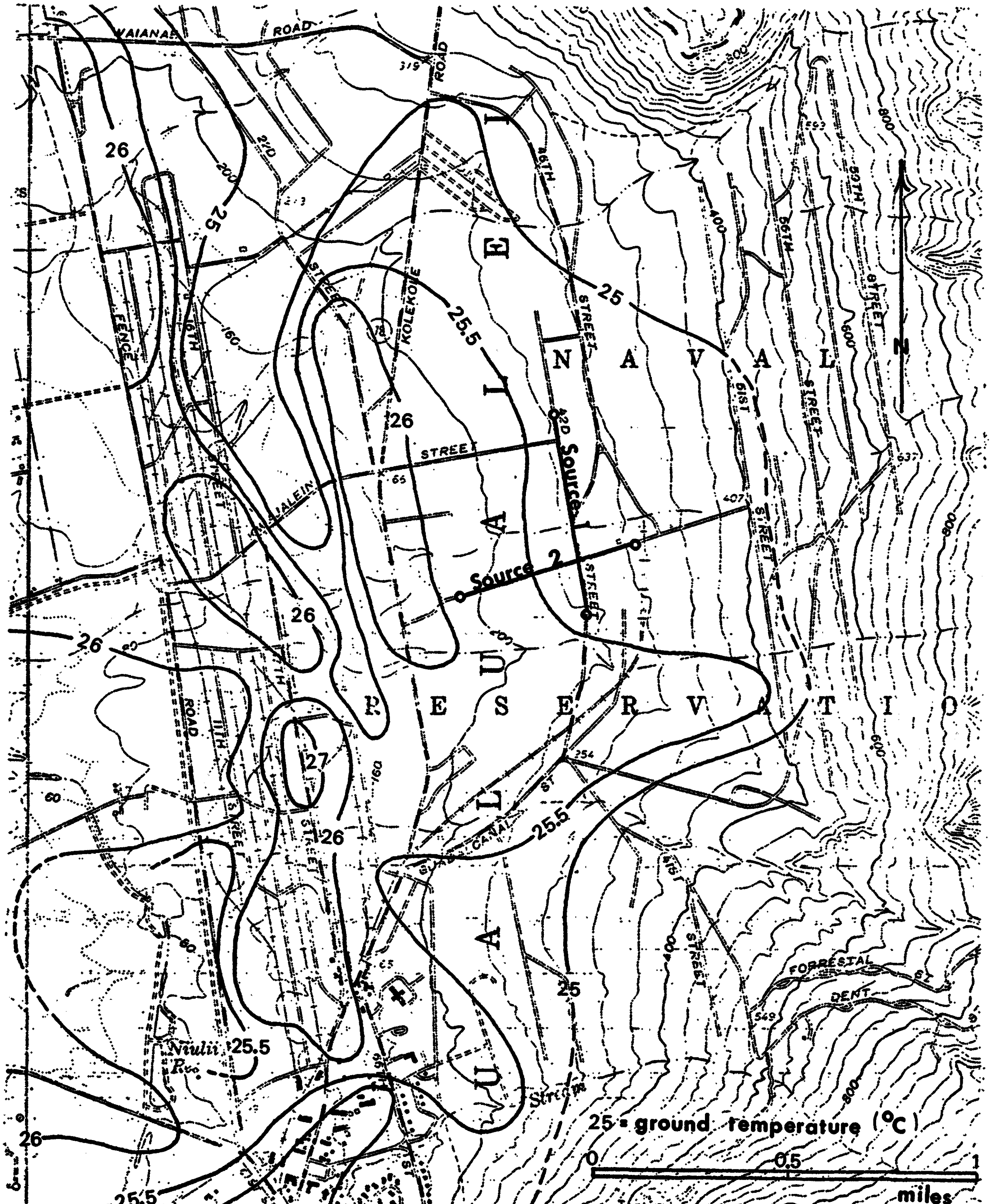

Figure 25. Ground temperature map of the Lualualei Naval Magazine, based on measurements made at 1 m depth

the area of interest, ending in an area with high resistivities. A loop was made around the anomaly to distribute the total error among individual measurements. A final self-potential line was run across the area with high anisotropy ratios (Fig. 23). The purpose was to see if the anisotropy in the area would be reflected in the self-potential measurements.

Interpretation of Field Data

Self-Potential: After error distribution (2 mv/200 m), potential drops with respect to the initial point with zero potential were calculated. Contoured self-potential values are shown in Figure 27. Self-potential over the area decreases, in general, to the north. The self-potential contours over the area where resistivity and temperature anomalies are located are distorted. The distortion might have been caused by movement of heated ground water that gives rise to streaming potentials.

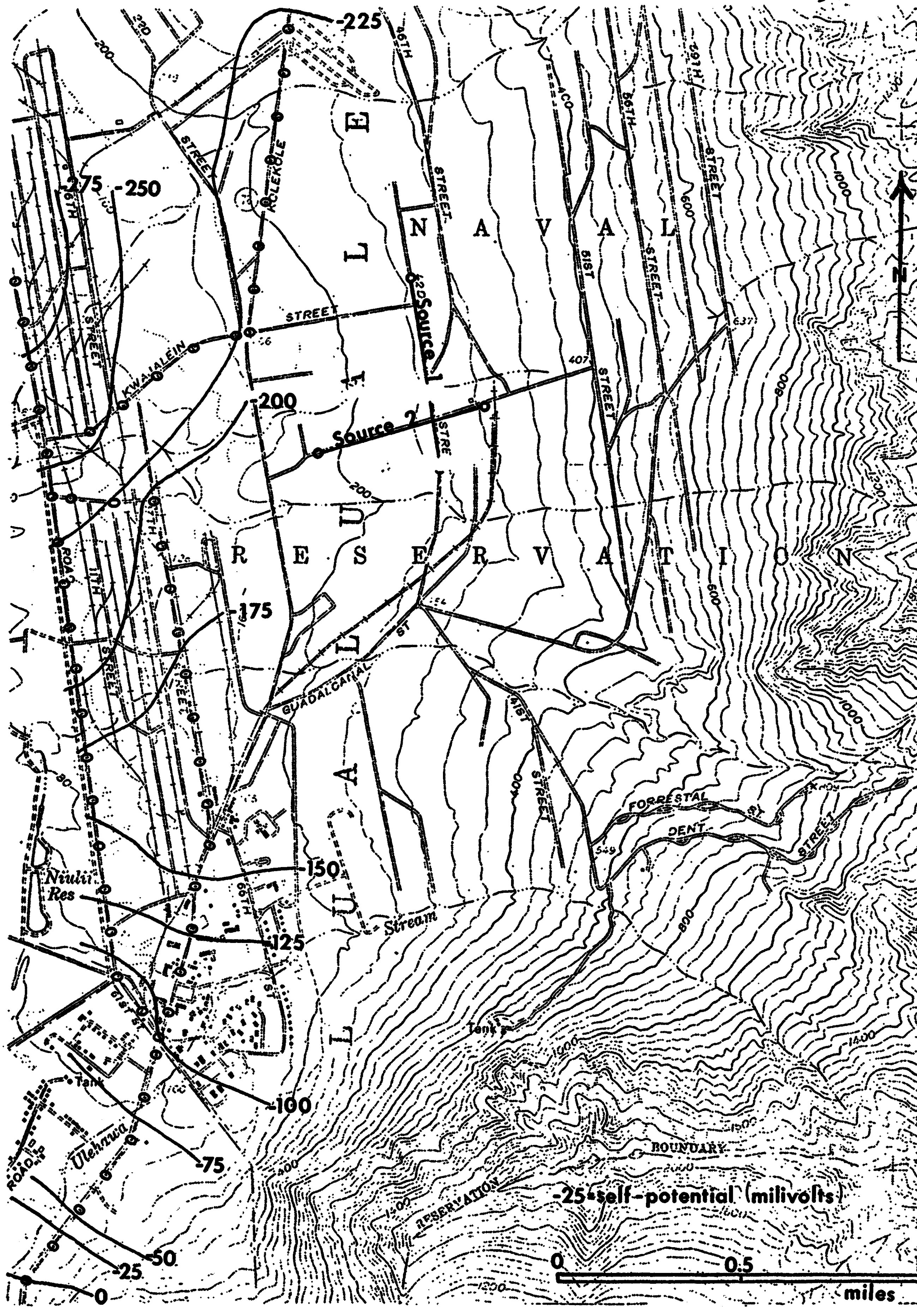

Figure 26. Self-potential map of the Lualualei Naval Magazine

RESULTS OF EVALUATION TECHNIQUES

Results of Rotating-Quadripole Survey

Using the rotating-quadripole method, the best apparent resistivity distribution of the study area was obtained (Fig. 17). As indicated by the resistivity distribution, the area does not have distinct layering; however, three zones with different resistivities in general, can be suggested. The alluvium on the surface is located above a zone with an intermediate apparent resistivity of about 50 ohm-m. High resistivities (higher than 75 ohm-m) indicate the presence of a resistive basement. Anomalous low resistivities (less than 30 ohm-m) were encountered in the area where Magazines 11 and 12 are located. These low resistivities could be the result of hot water saturated rocks at depth or a moderately thick section of clay rich alluvium. Contoured anisotropy ratios outlined the areas with anomalous anisotropies; thus, confirming the presence of a resistive basement and a conductive body at depth to the southwest of the area (Fig. 23).

Results of Temperature and Self-Potential Surveys

As a result of the temperature survey, areas with high ground temperatures were discovered (Fig. 24). An average temperature of 26.3°C in the area where anomalous low resistivities were detected, suggests the presence of a geothermal reservoir at depth. However, the other temperature anomalies are believed to be caused by local variations in the surface cover or by moving groundwater. The self-potential survey showed that the self-potential of the ground in the area, in general, decreases to the north (Fig. 26). The distortion on the self-potential contours over the area with low resistivities and high temperatures could be considered anomalous.

CONCLUSIONS AND RECOMMENDATIONS

Does the area where the Lualualei Naval Magazine is located have a geothermal reservoir? If so, does it contain high enthalpy water at an economical depth? These were the questions under consideration during the course of this study.

The area is located near a center of intense volcanism (Puu Kailio) inside the volcanic vent zone of the Waianae Caldera. Even though the Waianae Range was built in late Tertiary, the volcanism continued during the Quaternary period. Young volcanism in the area suggests the presence of a strong and active heat source. All geophysical work done in the area indicates the presence of a dense body of rock extending from shallow depths (800 m from the surface) to a depth of 5.5 km under the Waianae Caldera. It is probable that olivine and perhaps other heavy crystals that have lagged behind in basaltic magma rising toward the surface, and have accumulated to form a plug of peridotite that resembles mantle rock in its physical properties. The drill hole at the summit of Kilauea penetrated rocks with low permeability and densities around 3.2 gr/cc. The volcanic plug under the Waianae Caldera is believed to be made up of rocks similar to the rocks found under the Kilauea Volcano. Low permeability probably minimized the heat escape from the heat source; thus, maintaining its heat content over the years. The geological conditions in the area indicate the presence of a heat source.

The rocks located above the volcanic plug are believed to be highly fractured due to a high number of dikes of different sizes. Since these highly permeable basalts are located above the possible heat source, and since the area has abundant groundwater due to high rainfall, the section between the volcanic plug and the alluvial fill has the properties to behave as the reservoir rock for a geothermal system. The area where the anomaly is located may have up to 1000 feet of alluvium on the surface. The alluvium (Pleistocene) is believed to be partially consolidated and inasmuch as it is located above the permeable basalts, and there is a possibility of hydrothermal alteration, the alluvium could behave like a caprock because of its reduced permeability. Presence of a zone with low permeability over the reservoir minimizes the heat escape to the surface, keeping most of the heat in the reservoir, thus increasing the temperature of the groundwater. From the discussion above, it can be concluded that the geologic environment is suitable for presence of a geothermal system.

To locate the area with anomalous geothermal gradient, a rotating-quadripole survey was carried out. Anomalous low resistivities were discovered to the southwest of the dipole sources. A shallow temperature study which was done afterwards confirmed that the low resistivities were caused by high temperatures in the area. Because there is no surface activity, chemical analyses to determine the reservoir temperature were not available. Temperature measurements made at a meter depth could not be used to determine the true geothermal gradient.

As a result of this study, it is concluded that the area where magazines 11 and 12 are located may have a sealed geothermal reservoir at depth. However, the vertical resistivity distribution and the temperature gradient in the area are not known. A test hole which is deep enough to penetrate the basalts below the alluvium should be drilled to determine the temperature gradient and also to obtain valuable information about the rocks in the area. Perhaps a number of initial test holes with intermediate depths (20 m) could be drilled to determine the hottest part of the anomalous area.

APPENDIX I

DERIVATION OF APPARENT RESISTIVITY EXPRESSION FOR THE ROTATING-QUADRIPOLE ARRAY

Take two dipole sources at approximately right angles to each other. Even though it is desirable, they do not have to have a common electrode.

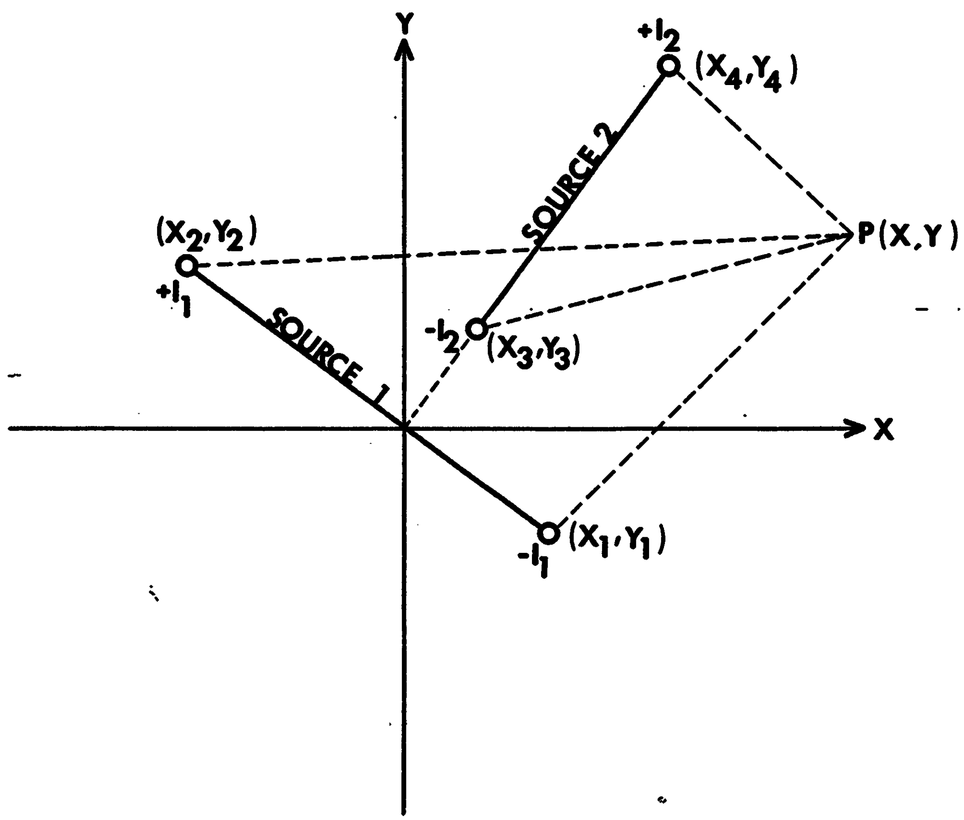

The potential expression for apparent resistivity assuming spherical current spreading from single electrode in a homogeneous earth is $u = \rho I/2\pi R$ (Van Nostrand and Cook, 1966). The potential at point P due to all four electrodes can be written.

$$U_1 = -\rho I_1/2\pi[(x-x_1)^2+(y-y_1)^2]^{1/2}$$

$$U_2 = +\rho I_1/2\pi[(x-x_2)^2+(y-y_2)^2]^{1/2}$$

$$U_3 = -\rho I_2/2\pi[(x-x_3)^2+(y-y_3)^2]^{1/2}$$

$$U_4 = +\rho I_2/2\pi[(x-x_4)^2+(y-y_4)^2]^{1/2}$$

Since $\vec{E} = -\vec{\nabla}U$, $E_x = -\partial U/\partial x$ and $E_y = -\partial U/\partial y$

x and y components of the electric field at point P due to all four electrodes:

$$E_{1x} = \rho I_1(x-x_1)/2\pi[(x-x_1)^2+(y-y_1)^2]^{3/2}$$

$$E_{1y} = \rho I_1(y-y_1)/2\pi[(x-x_1)^2+(y-y_1)^2]^{3/2}$$

$$E_{2x} = -\rho I_1(x-x_2)/2\pi[(x-x_2)^2+(y-y_2)^2]^{3/2}$$

$$E_{2y} = -\rho I_1(y-y_2)/2\pi[(x-x_2)^2+(y-y_2)^2]^{3/2}$$

$$E_{3x} = \rho I_2(x-x_3)/2\pi[(x-x_3)^2+(y-y_3)^2]^{3/2}$$

$$E_{3y} = \rho I_2(y-y_3)/2\pi[(x-x_3)^2+(y-y_3)^2]^{3/2}$$

$$E_{4x} = -\rho I_2(x-x_4)/2\pi[(x-x_4)^2+(y-y_4)^2]^{3/2}$$

$$E_{4y} = -\rho I_2(y-y_4)/2\pi[(x-x_4)^2+(y-y_4)^2]^{3/2}$$

The total electric fields in x and y directions are:

$$E_{Tx} = \frac{\rho}{2\pi}\left\{\frac{I_1\ (x-x_1)}{[(x-x_1)^2+(y-y_1)^2]^{3/2}} - \frac{I_1\ (x-x_2)}{[(x-x_2)^2+(y-y_2)^2]^{3/2}}\right.$$

$$\left. + \frac{I_2\ (x-x_3)}{[(x-x_3)^2+(y-y_3)^2]^{3/2}} - \frac{I_2(x-x_4)}{[(x-x_4)^2+(y-y_4)^2]^{3/2}}\right\}$$

$$E_{Ty} = \frac{\rho}{2\pi} \{\frac{I_1\ (y-y_1)}{[(x-x_1)^2+(y-y_1)^2]^{3/2}} - \frac{I_1\ (x-x_2)}{[(x-x_2)^2+(y-y_2)^2]^{3/2}}$$

$$+ \frac{I_2\ (y-y_3)}{[(x-x_3)^2+(y-y_3)^2]^{3/2}} - \frac{I_2\ (y-y_4)}{[(x-x_4)^2+(y-y_4)^2]^{3/2}}\}$$

The amplitude of the total electric field at point P is:

$$E_{TOT} = (E_{Tx}^2 + E_{Ty}^2)^{1/2}$$

Let:

$$R_1 = [(x-x_1)^2 + (y-y_1)^2]^{1/2}$$

$$R_2 = [(x-x_2)^2 + (y-y_2)^2]^{1/2}$$

$$R_3 = [(x-x_3)^2 + (y-y_3)^2]^{1/2}$$

$$R_4 = [(x-x_4)^2 + (y-y_4)^2]^{1/2}$$

Substitute four equations above in the equation for E_{TOT}

$$E_{TOT} = \frac{\rho}{2\pi} \{[\frac{I_1(x-x_1)}{R_1{}^3} - \frac{I_1(x-x_2)}{R_2{}^3} + \frac{I_2(x-x_3)}{R_3{}^3} - \frac{I_2(x-x_4)}{R_4{}^3}]^2$$

$$+ [\frac{I_1(y-y_1)}{R_1{}^3} - \frac{I_1(x-x_2)}{R_2{}^3} + \frac{I_2(y-y_3)}{R_3{}^3} - \frac{I_2(y-y_4)}{R_4{}^3}]^2\}^{1/2}$$

$$E_{TOT} = \frac{\rho}{2\pi} \{ \frac{I_1{}^2(x-x_1)^2}{R_1{}^6} + \frac{I_1{}^2(x-x_2)^2}{R_2{}^6} + \frac{I_2(x-x_3)^2}{R_3{}^6} + \frac{I_2(x-x_4)^2}{R_4{}^6}$$

$$- \frac{2I_1{}^2(x-x_1)(x-x_2)}{R_1{}^3R_2{}^3} + \frac{2I_1I_2(x-x_1)(x-x_3)}{R_1{}^3R_3{}^3}$$

$$- \frac{-2I_1I_2(x-x_1)(x-x_4)}{R_1{}^3R_4{}^3} - \frac{-2I_1I_2(x-x_2)(x-x_3)}{R_2{}^3R_3{}^3}$$

$$+ \frac{2I_1I_2(x-x_2)(x-x_4)}{R_2{}^3R_4{}^3} - \frac{2I_2{}^2(x-x_3)(x-x_4)}{R_3{}^3R_4{}^3}$$

$$+ \frac{I_1{}^2(y-y_1)^2}{R_1{}^6} + \frac{I_1{}^2(y-y_2)^2}{R_2{}^6} + \frac{I_2{}^2(y-y_3)^2}{R_3{}^6}$$

$$+ \frac{I_2{}^2(y-y_4)}{R_4{}^6} - \frac{2I_1{}^2(y-y_1)(y-y_2)}{R_1{}^3R_2{}^3}$$

$$+ \frac{2I_1I_2(y-y_1)(y-y_3)}{R_1{}^3R_3{}^3} - \frac{2I_1I_2(y-y_1)(y-y_4)}{R_1{}^3R_4{}^3}$$

$$- \frac{2I_1I_2(y-y_2)(y-y_3)}{R_2{}^3R_3{}^3} + \frac{2I_1I_2(y-y_2)(y-y_4)}{R_2{}^3R_4{}^3}$$

$$- \frac{2I_2{}^2(y-y_3)(y-y_4)}{R_3{}^3R_4{}^3} \}^{1/2}$$

$$
\begin{aligned}
E_{TOT} = \frac{\rho}{2\pi} \Big\{ & \frac{I_1^{\,2}}{R_1^{\,6}} [(x-x_1)^2+(y-y_1)^2] + \frac{I_1^{\,2}}{R_2^{\,6}} [(x-x_2)^2+(y-y_2)^2] \\
& + \frac{I_2^{\,2}}{R_3^{\,6}} [(x-x_3)^2+(y-y_3)^2] + \frac{I_2}{R_4^{\,6}} [(x-x_4)^2+(y-y_4)^2] \\
& - \frac{2I_1^{\,2}}{R_1^{\,3}R_2^{\,3}} [(x-x_1)(x-x_2) + (y-y_1)(y-y_2)] \\
& - \frac{2I_1I_2}{R_1^{\,3}R_3^{\,3}} [(x-x_1)(x-x_3) + (y-y_1)(y-y_3)] \\
& - \frac{2I_1I_2}{R_1^{\,3}R_4^{\,3}} [(x-x_1)(x-x_4) + (y-y_1)(y-y_4)] \\
& - \frac{2I_1I_2}{R_2^{\,3}R_3^{\,3}} [(x-x_2)(x-x_3) + (y-y_2)(y-y_3)] \\
& + \frac{2I_1I_2}{R_2^{\,3}R_4^{\,3}} [(x-x_2)(x-x_4) + (y-y_2)(y-y_4)] \\
& - \frac{2I_2}{R_3^{\,3}R_4^{\,3}} [(x-x_3)(x-x_4) + (y-y_3)(y-y_4)]\Big\}^{1/2}
\end{aligned}
$$

Let: $C = I_1/I_2$ and substitute this equation in the last equation for E_{TOT} above.

$$E_{TOT} = \frac{\rho I_2}{2\pi} \{ \frac{C^2}{R_1^{\,4}} + \frac{C^2}{R_2^{\,4}} + \frac{1}{R_3^{\,4}} + \frac{1}{R_4^{\,4}}$$

$$- \frac{2C^2}{R_1^{\,3} R_2^{\,3}} [(x-x_1)(x-x_2) + (y-y_1)(y-y_2)]$$

$$+ \frac{2C}{R_1^{\,3} R_3^{\,3}} [(x-x_1)(x-x_3) + (y-y_1)(y-y_3)]$$

$$- \frac{2C}{R_1^{\,3} R_4^{\,3}} [(x-x_1)(x-x_4) + (y-y_1)(y-y_4)]$$

$$- \frac{2C}{R_2^{\,3} R_3^{\,3}} [(x-x_2)(x-x_3) + (y-y_2)(y-y_3)]$$

$$+ \frac{2C}{R_2^{\,3} R_4^{\,3}} [(x-x_2)(x-x_4) + (y-y_2)(y-y_4)]$$

$$- \frac{2}{R_3^{\,3} R_4^{\,3}} [(x-x_3)(x-x_4) + (y-y_3)(y-y_4)]\}^{1/2}$$

Call that part of the equation in parentheses K.

$$E_{TOT} = \frac{\rho I_2}{2\pi} K, \quad \rho = \frac{2\pi E_{TOT}}{I_2 K} .$$

The expression for apparent resistivity is

$$\rho = \frac{2\pi E_{TOT}}{I_2 K}$$

where K is the geometric factor. To find the apparent resistivity expressions for dipoles one and two individually, let $I_2 = 0$ and $I_1 = 0$ respectively in the composite equation for the rotating-quadripole array above.

Let:

$$I_2 = 0$$

$$E_{TOT_1} = \frac{\rho I_1}{2\pi} \left\{\frac{1}{R_1^{\,4}} + \frac{1}{R_2^{\,4}} - \frac{2}{R_1^{\,3} R_2^{\,3}} \left[(x-x_1)(x-x_2)+(y-y_1)(y-y_2)\right]\right\}^{1/2}$$

$$E_{TOT_1} = \frac{\rho I_1}{2\pi} K_1$$

$\rho = \dfrac{2\pi E_{TOT_1}}{I_1 K_1}$: Apparent resistivity equation for the first source.

Let:

$$I_1 = 0$$

$$E_{TOT_2} = \frac{\rho I_2}{2\pi} \left\{\frac{1}{R_3^{\,4}} + \frac{1}{R_4^{\,4}} - \frac{2}{R_3^{\,3} R_4^{\,3}} \left[(x-x_3)(x-x_4)+(y-y_3)(y-y_4)\right]\right\}^{1/2}$$

$$E_{TOT_2} = \frac{\rho I_2}{2\pi} K_2$$

$\rho = \dfrac{2\pi E_{TOT_2}}{I_2 K_2}$: Apparent resistivity equation for the second source.

APPENDIX II

DESCRIPTION OF THE COMPUTER PROGRAM

For every station, the direction and the amplitude of the two total electric fields are calculated. ET_1 for source #1 and ET_2 for source #2.

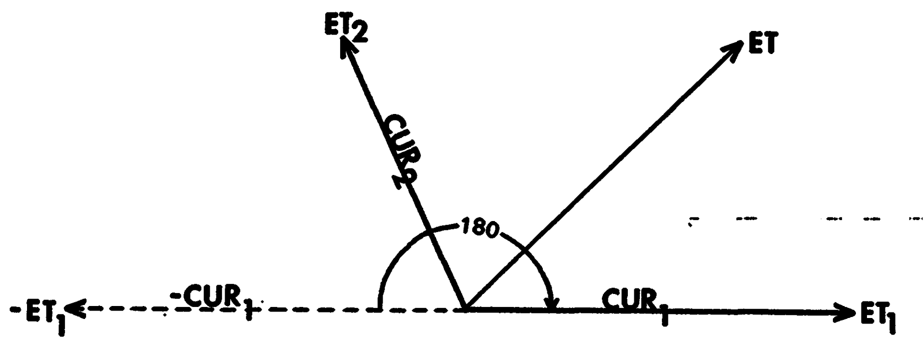

If sources #1 and #2 were both turned on, the new total electric field ET would have a different direction and amplitude than ET_1 and ET_2. The vector ET is the resultant of the two independent vectors ET_1 and ET_2. There exists a linear relationship between the current on a source and the amplitude of the electric field at a point, created by that source. Total step currents on both sources can be varied to control the direction of ET.

The program changes the sign on the current for source #1. This changes the sign on ET_1 and the direction 180°. Then, CUR1 (current on source #1) is increased from -CUR1 to zero and CUR2 (current on source #2) is also increased from zero to CUR2. So far, ET is rotated from the direction of $-ET_1$ to the direction of ET_2. To complete the rotation of ET from -ET1 to ET1 (180°), CUR2 is decreased from CUR2 to zero and CUR1 is increased from zero to CUR1. The currents are varied 5% at a time and the direction and the amplitude of ET is determined from the new amplitudes and directions of ET1 and ET2. Since the geometric factor K is also a function of CUR1 and CUR2, for every current change a new geometric factor was calculated. See Appendix I for the geometric factor expression K.

Resistivities were calculated using the apparent resistivity expression for the rotating-quadripole method. Output includes 41 sets of values for electric-field bearings, total electric fields and resistivities for every recording station (see the next page). The first and last resistivity values are the same and it is the resistivity from source #1 alone, for -ET1 and ET1. The twenty-first set of values are from source #2 alone, and out of these 40 different resistivity values the maximum and the minimum are picked out.

See the next page for a sample of the output and the last four pages in this Appendix for the computer program.

PROJECT 307.LLL.HAWAII

STATION NUMBER 1 AT A DISTANCE OF 0.021 KILOMETERS
TOTAL FIELD 1 IS [illegible].619E+23 MICROVOLTS AT A BEARING OF 11. DEGREES
TOTAL FIELD 2 IS [illegible].433E+23 MICROVOLTS AT A BEARING OF 93. DEGREES

E FIELD BEARING	TOTAL E FIELD	RESISTIVITY, OHM-METERS	
191.	618.68	26.46	**Source 1**
189.	585.14	26.51	
186.	552.47	26.58	
184.	520.85	26.68	
181.	490.49	26.83	
177.	461.62	27.03	
173.	434.55	27.30	
169.	409.63	27.67	
164.	387.29	28.15	
159.	367.98	28.77	
153.	352.21	29.54	
147.	340.47	30.46	
140.	333.18	31.50	
133.	330.65	32.56	
126.	332.98	33.54	
119.	340.06	34.32	
113.	351.62	34.80	
107.	367.23	34.99	**Maximum Resistivity**
102.	386.40	34.91	
97.	408.62	34.65	
93.	433.44	34.29	**Source 2**
88.	417.19	33.82	
84.	403.36	33.23	
79.	392.22	32.53	
74.	384.00	31.76	
69.	378.89	30.94	
63.	377.01	30.14	
58.	378.42	29.38	
53.	383.07	28.70	
48.	390.85	28.12	
43.	401.58	27.64	
38.	415.04	27.25	
34.	430.95	26.96	
30.	449.08	26.74	
27.	469.15	26.59	
23.	490.92	26.49	
20.	514.20	26.43	
17.	538.77	26.41	**Minimum Resistivity**
15.	564.47	26.41	
13.	591.15	26.43	
11.	618.68	26.46	**Source 1**

Computer output from the rotating-quadripole program for station 1

```
C ********************** QDPL.F4 **********************
C QDPL.F4 IS A PROGRAM TO COMPILE ROTATING DIPOLE INFORMATION
C FROM FIELD MEASUREMENTS MADE WITH THE CROSSED DIPOLE ARRAY.
C VERSION OCTOBER 22,1974.
C INPUT DATA CONSISTS OF
C   1. A HEADER CARD IN ALPHANUMERIC FORMAT
C   2. A CARD IN 9F FORMAT WITH THE COORDINATES OF THE FOUR
C      POLES AND THE RECEIVER LENGTH.THE INTERSECTION POINT
C      OF THE TWO SOURCES IS THE ORIGIN.E-W LINE IS THE X-
C      AXIS(EAST IS THE POSITIVE DIRECTION).N-S LINE IS THE
C      Y-AXIS(NORTH IS THE POSITIVE DIRECTION).
C      X1,Y1: NEGATIVE ELECTRODE ,SOURCE 1
C      X2,Y2: POSITIVE ELECTRODE ,SOURCE 1
C      X3,Y3: NEGATIVE ELECTRODE ,SOURCE 2
C      X4,Y4: POSITIVE ELECTRODE ,SOURCE 2
C      XL, THE LENGTH OF THE RECEIVER LINE
C      THE PROPER CRDER: X1,X2,X3,X4,Y1,Y2,Y3,Y4,XL
C   3. A SERIES OF CARDS WITH DATA FOR INDIVIDUAL STATIONS
C      N, THE STATION NUMBER
C      R, THE DISTANCE FROM THE ORIGIN
C      BEAR, THE BEARING OF LINE TO RECEIVER
C      B1,EX1: THE BEARING,THE VOLTAGE,LINE ONE,SOURCE 1
C      B2,EY2: THE BEARING,THE VOLTAGE,LINE TWO,SOURCE 1
C      BR1,EX2: THE BEARING,THE VOLTAGE,LINE ONE,SOURCE 2
C      BR2,EY2: THE BEARING,THE VOLTAGE,LINE TWO,SOURCE 2
C      CUR1, THE CURRENT FOR SOURCE 1
C      CUR2, THE CURRENT FOR SOURCE 2
C      THE PROPER CRDER: N,R,BEAR,B1,B2,BR1,BR2,EX1,EY1,EX2,
C      EY2,CUR1,CUR2
C   4. A FINAL CARD WHICH IS BLANK OR HAS A NEGATIVE NUMBER
C ****************************************************************
      DIMENSION A(20)
      READ (1,1000) (A(I),I=1,20)
1000  FORMAT (20A4)
      WRITE (2,1001) (A(I),I=1,20)
1001  FORMAT (///,20A4)
      READ (1,1002) X1,X2,X3,X4,Y1,Y2,Y3,Y4,XL
1002  FORMAT (9F)
103   CONTINUE
      READ (1,1003) N,R,BEAR,B1,B2,BR1,BR2,EX1,EY1,EX2,EY2,CUR1,CUR2
1003  FORMAT (I,12F)
      IF (N) 1,1,2
1     GO TO 103
2     CONTINUE
C****************************************************************
C THE FOLLOWING SEGMENT MAKES ALL THE VOLTAGES POSITIVE AND
C CORRECTS THE BEARINGS.
C****************************************************************
      IF (EX1) 401,402,402
401   EX1=-EX1
      B1=B1+180.
      IF (B1.GT.360.) B1=B1-360.
402   IF (EY1) 403,404,404
403   EY1=-EY1
      B2=B2+180.
      IF (B2.GT.360.) B2=B2-360.
404   IF (EX2) 405,406,406
405   EX2=-EX2
      BR1=BR1+180.
      IF (BR1.GT.360.) BR1=BR1-360.
```

```
406       IF (EY2) 407,408,408
407       EY2=-EY2
          BR2=BR2+180.
          IF (BR2.GT.360.) BR2=BR2-360.
C ******************************************************************
C THIS SEGMENT REARRENGES VOLTAGES SO THAT B1<B2 AND BR1<BR2
C THETA (FIRST SOURCE) AND THETA2 (SECOND SOURCE) ARE THE
C ANGLES BETWEEN THE TWO RECEIVER LINES,POSITIVE AND LESS
C THAN 180 DEGREES.
C ******************************************************************
400       IF (B1-B2) 6,7,7
6         GO TO 10
7         TEX1=EX1
          EX1=EY1
          EY1=TEX1
          TB1=B1
          B1=B2
          B2=TB1
10        THETA=(B2-B1)/57.29573
          EX1=EX1/XL
          EY1=EY1/XL
          EY1=(EY1-EX1*COS(THETA))/SIN(THETA)
          ET1=SQRT(EX1*EX1+EY1*EY1)
          YT=EX1*SIN(B1/57.29573)+EY1*SIN(B2/57.29573)
          XT=EX1*COS(B1/57.29573)+EY1*COS(B2/57.29573)
          IF (XT.GT.0..AND.YT.GT.0.) B3=ATAN(YT/XT)
          IF (XT.LT.0..AND.YT.GT.0.) B3=1.570796+ATAN(-XT/YT)
          IF (XT.LT.0..AND.YT.LT.0.) B3=3.141592+ATAN(YT/XT)
          IF (XT.GT.0..AND.YT.LT.0.) B3=4.712388+ATAN(-XT/YT)
          IF (XT.EQ.0..AND.YT.GT.0.) B3=1.570796
          IF (XT.EQ.0..AND.YT.LT.0.) B3=4.712388
          IF (XT.GT.0..AND.YT.EQ.0.) B3=0.
          IF (XT.LT.0..AND.YT.EQ.0.) B3=3.141592
          IF (BR1-BR2) 8,9,9
8         GO TO 11
9         TEX2=EX2
          EX2=EY2
          EY2=TEX2
          TBR1=BR1
          BR1=BR2
          BR2=TBR1
11        THETA2=(BR2-BR1)/57.29573
          EX2=EX2/XL
          EY2=EY2/XL
          EY2=(EY2-EX2*COS(THETA2))/SIN(THETA2)
          ET2=SQRT(EX2*EX2+EY2*EY2)
          YY=EX2*SIN(BR1/57.29573)+EY2*SIN(BR2/57.29573)
          XX=EX2*COS(BR1/57.29573)+EY2*COS(BR2/57.29573)
          IF (XX.GT.0..AND.YY.GT.0.) B4=ATAN(YY/XX)
          IF (XX.LT.0..AND.YY.GT.0.) B4=1.570796+ATAN(-XX/YY)
          IF (XX.LT.0..AND.YY.LT.0.) B4=3.141592+ATAN(YY/XX)
          IF (XX.GT.0..AND.YY.LT.0.) B4=4.712388+ATAN(-XX/YY)
          IF (XX.EQ.0..AND.YY.GT.0.) B4=1.570796
          IF (XX.EQ.0..AND.YY.LT.0.) B4=4.712388
          IF (XX.GT.0..AND.YY.EQ.0.) B4=0.0
          IF (XX.LT.0..AND.YY.EQ.0.) B4=3.141592
          XB3=B3*57.29573
          XB4=B4*57.29573
C ******************************************************************
C ET1 AND ET2 ARE THE MAGNITUDES OF THE TWO TOTAL FIELDS.
```

```
C CONSIDERING THAT THE ANGLE  BETWEEN RECEIVERS IS NOT
C NECESSARILY 90 DEGREES. B3 AND B4 ARE THE BEARINGS OF THE
C TWO TOTAL FIELD VECTORS.
C ***********************************************************
      WRITE (2,1034) N,R,ET1,XB3,ET2,XB4
1034  FORMAT (/,1X,'STATION NUMBER ',I3,' AT A DISTANCE OF ',
     6 F6.3,' KILOMETERS',/,1X,'TOTAL FIELD 1 IS ',E10.3,
     6 ' MICROVOLTS AT A BEARING OF ',F4.0,' DEGREES',/,1X,
     6 'TOTAL FIELD 2 IS ',E10.3,' MICROVOLTS AT A BEARING OF '
     6 ,F4.0,' DEGREES',//,9X,'E FIELD',10X,'TOTAL',10X,
     6 'RESISTIVITY,',/,9X,'BEARING',10X,'E FIELD',8X,
     6 'OHM-METERS',/)
C ***********************************************************
C THIS SEGMENT VARIES THE CURRENTS ON BOTH SOURCES AND CALCULATES
C THE AMPLITUDE AND THE DIRECTION OF THE E FIELD, THE GEOMETRIC
C FACTORS AND THE RESISTIVITIES.
C ***********************************************************
      DO 101 J=1,41
      FC=J-21
      CR1=CUR1*FC*.05
      IF (J.GT.21) GO TO 115
      FD=J-1
      CR2=CUR2*FD*.05
      GO TO 116
115   FD=41-J
      CR2=CUR2*FD*.05
116   ET1COR=ET1*FC*.05
      ET2COR=ET2*FD*.05
      CX=ET1COR*SIN(B3)+ET2COR*SIN(B4)
      CY=ET1COR*COS(B3)+ET2COR*COS(B4)
      ET=SQRT(CX*CX+CY*CY)
      IF (CR1.EQ.0.) BT=B4
      IF (CR2.EQ.0.) BT=B3
      IF (CX.GT.0..AND.CY.GT.0.) BT=ATAN(CX/CY)
      IF (CX.GT.0..AND.CY.LT.0.) BT=1.570796+ATAN(-CY/CX)
      IF (CX.LT.0..AND.CY.LT.0.) BT=3.141592+ATAN(CX/CY)
      IF (CX.LT.0..AND.CY.GT.0.) BT=4.712388+ATAN(-CY/CX)
      BT=BT*57.29573
      X=R*SIN(BEAR/57.29573)
      Y=R*COS(BEAR/57.29573)
      XX1=X-X1
      XX2=X-X2
      XX3=X-X3
      XX4=X-X4
      YY1=Y-Y1
      YY2=Y-Y2
      YY3=Y-Y3
      YY4=Y-Y4
      R1=SQRT(XX1*XX1+YY1*YY1)
      R2=SQRT(XX2*XX2+YY2*YY2)
      R3=SQRT(XX3*XX3+YY3*YY3)
      R4=SQRT(XX4*XX4+YY4*YY4)
      IF (CR2) 111,111,112
111   GEOM=SQRT(R1**-4.+R2**-4.-(2.*(XX1*XX2+YY1*YY2)/(R1**3.*R2**3.)))
      RES=(6.283185*ET1COR)/(CR1*GEOM)
      GO TO 113
112   CR12=CR1/CR2
      T1=(CR12**2.)/(R1**4.)+CR12**2./R2**4.+R3**-4.+R4**-4.
      T2=((-2.*CR12**2.)/(R1**3.*R2**3.))*(XX1*XX2+YY1*YY2)
      T3=(2.*CR12/(R1**3.*R3**3.))*(XX1*XX3+YY1*YY3)
```

```
      T4=(-2.*CR12/(R1**3.*R4**3.))*(XX1*XX4+YY1*YY4)
      T5=(-2.*CR12/(R2**3.*R3**3.))*(XX2*XX3+YY2*YY3)
      T6=(2.*CR12/(R2**3.*R4**3.))*(XX2*XX4+YY2*YY4)
      T7=(-2./(R3**3.*R4**3.))*(XX3*XX4+YY3*YY4)
      GEOM1=T1+T2+T3+T4+T5+T6+T7
      GEOM=SQRT(GEOM1)
      RES=(6.2831853*ET)/(CR2*GEOM)
113   WRITE (2,1008) BT,ET,RES
1008  FORMAT (10X,F4.0,10X,F8.2,10X,F8.2)
101   CONTINUE
      GO TO 100
103   CONTINUE
      STOP
      END
```

APPENDIX III

ROTATING-QUADRIPOLE MAPPING FIELD DATA

N : Station number

R : Distance from measuring point to the origin (the intersection point of the two sources)(km)

BEAR: Azimuth of the line between the origin and the receiver station (degrees)

B1 : Azimuth of the first receiver line (source #1)(degrees)

B2 : Azimuth of second receiver line (source #1)(degrees)

BR1 : Azimuth of first receiver line (source #2)(degrees)

BR2 : Azimuth of second receiver line (source #2)(degrees)

EX1 : Voltage measured along first receiver line (source #1)(mv)

EY1 : Voltage measured along second receiver line (source #1)(mv)

EX2 : Voltage measured along first receiver line (source #2) (mv)

EY2 : Voltage measured along second receiver line (source #2)(mv)

CUR1: Total step current on source #1 (amperes)

CUR2: Total step current on source #2 (amperes)

XL : Length of receiver line (meters)

R1 : Resistivity due to source #1 (ohm-m)

R2 : Resistivity due to source #2 (ohm-m)

Rmax: Maximum resistivity (ohm-meters)

Rmin: Minimum resistivity (ohm-meters)

RTO : Ratio of maximum to minimum resistivity

N	R	BEAR	B1	B2	BR1	BR2	EX1	EY1	EX2	EY2	CUR1	CUR2	XL	R1	R2	R_{max}	R_{min}	RTO
1	0.021	112	186	287	180	256	-18500	5000	-6500	-12500	4.5	3.5	30	26.5	34.3	35.0	26.4	1.3
2	1.067	351	174	76	175	75	3200	-140	260	400	4.5	3.5		31.3	58.9	51.0	27.0	1.9
3	0.591	8	167	74	76	170	-9040	-10100	775	1300	4.5	3.5		23.2	33.2	32.0	14.0	2.3
4	0.747	75	174	75	171	75	-1200	225	650	-2100	4.5	3.8		41.1	35.5	62.2	26.4	2.4
5	0.344	55	350	100	353	84	9240	-1200	-68000	-10500	4.5	3.5		70.9	70.9	118.7	71.1	1.7
6	0.850	52	172	84	171	85	-1300	-1750	1750	1000	4.6	3.8		71.0	53.7	82.0	19.1	4.3
7	1.079	35	20	329	326	20	-675	-625	-1650	-500	4.6	3.8		25.1	116.6	113.9	17.7	5.8
8	1.487	21	350	78	349	72	-240	-240	-260	40	4.6	3.8		21.8	49.4	52.4	19.6	2.7
9	1.378	30	172	78	172	74	-60	-800	260	-70	4.6	3.8		52.4	35.8	60.2	34.6	1.7
10	1.716	28	75	169	158	67	-580	50	230	-80	4.6	3.8		71.5	63.0	84.4	61.4	1.4
11	1.975	22	330	355	11	342	-90	-150	-180	-160	4.6	3.8		31.9	74.6	76.1	4.0	19.2
12	1.301	43	238	1	348	358	260	130	-300	-320	4.6	4.0		46.7	32.8	51.7	3.7	13.8
13	1.106	60	350	72	350	75	640	-220	-265	-470	4.6	4.0		54.1	28.8	54.5	28.0	2.0
14	1.036	79	349	80	75	348	480	55	-650	65	4.6	4.0		36.5	29.2	41.3	28.4	1.5
15	1.320	118	325	353	328	353	-60	40	170	140	4.6	4.0		22.3	19.0	23.2	10.9	2.1
16	1.116	99	173	180	175	180	-275	-350	-370	-300	4.6	4.0		57.3	52.8	60.8	7.4	8.2
17	1.350	82	355	35	6	353	350	290	-7	45	4.6	4.0		54.3	26.3	61.4	21.9	2.8
18	1.414	64	143	173	182	149	-360	-320	142	20	4.6	4.0		57.3	25.9	60.2	14.3	4.2
19	1.582	50	169	180	180	167	-250	-160	142	120	4.6	3.9		82.9	28.1	83.9	10.5	8.0
20	1.789	40	169	84	168	82	-45	-270	270	-105	4.6	3.9		50.2	75.0	84.2	50.4	1.7
21	2.103	31	171	76	75	170	90	-200	-65	165	4.6	3.9		53.6	75.1	77.6	46.2	1.7
22	2.335	25	14	101	94	10	-140	-90	20	-95	4.6	3.9		50.9	62.3	63.9	46.3	1.4
23	0.860	111	350	6	5	349	370	560	850	1075	4.6	3.8		30.6	41.9	53.1	29.9	1.8
24	1.100	129	349	89	349	77	-180	460	480	-40	4.5	3.8		30.0	39.5	46.5	29.4	1.6
25	1.487	137	289	211	295	203	-170	-15	50	-185	4.5	3.8		23.1	38.6	60.0	17.8	3.4
26	1.189	148	106	18	105	12	-350	-125	60	345	4.5	3.8		25.3	39.5	47.1	24.7	1.9
27	0.978	161	105	120	107	118	460	590	390	300	4.5	3.8		27.7	47.1	47.9	25.7	1.9
28	0.850	178	284	299	285	298	925	300	-460	-370	4.5	3.8		62.4	29.7	68.1	23.9	2.9
29	1.250	168	310	20	22	312	-950	-900	425	625	4.5	3.8		131.4	102.0	122.1	71.3	1.7
30	1.631	162	345	65	345	65	-250	-30	85	210	4.5	3.8		39.7	69.6	77.0	38.9	2.0
31	2.111	163	343	74	348	77	-130	-15	65	150	4.5	3.8		42.7	111.2	120.0	40.2	3.0
32	1.890	159	346	77	346	80	-180	45	60	160	4.5	3.8		46.7	86.0	107.6	29.4	3.7
33	2.118	144	139	246	140	246	110	-50	-10	-65	4.5	3.8		38.9	42.7	83.4	12.2	6.8
34	2.341	135	45	87	43	85	43	60	50	15	4.5	3.8		29.4	43.2	72.2	20.9	3.5
35	2.131	155	190	235	232	196	70	4	-110	-90	4.5	3.8		32.5	75.2	81.4	33.3	2.4

N	R	BEAR	B1	B2	BR1	BR2	EX1	EY1	EX2	EY2	CUR1	CUR2	XL	R1	R2	R_{max}	R_{min}	RTO
36	2.454	142	300	200	300	202	-40	-12	-20	-70	4.5	3.8	30	24.3	71.1	94.5	18.3	5.2
37	2.630	127	239	216	263	239	-45	-35	11	-7	4.5	3.8		40.5	40.7	85.6	12.0	7.1
38	0.433	176	183	99	92	181	8250	-850	1900	-1550	4.5	3.8		23.8	31.7	33.1	17.0	1.9
39	0.378	134	182	101	179	90	2900	8300	-4700	1800	4.5	3.8		23.6	31.2	41.3	14.4	2.9
40	0.323	351	171	181	170	180	-8000	-7700	1800	1150	4.5	3.5		26.1	34.1	62.9	1.8	34.8
41	2.469	163	40	53	61	46	-20	-12	130	120	4.55	3.8		22.5	134.8	151.7	7.1	21.5
42	2.719	171	227	244	229	244	-50	-80	-75	-85	4.55	3.8		79.9	120.9	147.4	8.5	17.3
43	1.125	196	55	140	149	58	-530	110	250	220	4.55	3.7		31.6	25.4	43.7	19.1	2.3
44	1.372	360	189	198	198	188	1150	1100	90	150	4.6	3.5		38.9	72.8	111.2	9.9	11.3
45	2.112	352	141	33	124	35	330	-300	100	10	4.5	3.5		66.3	73.7	77.5	53.9	1.4
46	1.719	354	342	68	342	72	-730	-35	-190	240	4.5	3.5		58.2	124.5	125.9	50.2	2.5
47	2.070	343	190	105	105	189	190	490	280	-60	4.5	3.5		81.5	210.1	212.2	40.7	5.2
48	2.438	347	189	205	205	188	120	28	-50	0	4.5	3.9		96.7	175.0	233.2	43.3	5.4
49	2.661	344	121	79	120	79	275	140	52	90	4.5	3.9		111.8	121.0	143.2	65.3	2.2
50	2.835	354	227	200	204	230	80	115	7	-25	4.5	3.8		59.4	108.7	115.5	10.0	11.5
51	2.963	348	281	255	281	255	90	12	-42	-35	4.5	3.8		99.1	77.4	151.3	13.8	10.9
52	3.127	357	127	65	126	66	65	-60	18	12	4.5	3.8		79.6	39.1	99.9	33.2	3.0
53	2.713	360	306	325	312	336	-145	-167	-48	-32	4.5	3.8		69.5	71.7	82.1	38.1	2.2
54	2.377	6	314	334	315	333	-130	-170	-90	-75	4.5	3.8		51.9	80.3	82.0	21.4	3.8
55	2.393	16	186	215	217	238	155	180	30	-28	4.5	3.8		55.7	119.7	125.2	19.4	6.4
56	2.393	339	114	129	100	116	140	170	90	60	4.5	3.7		53.5	130.6	143.8	45.5	3.2
57	1.250	313	168	81	172	77	950	1850	-145	220	4.5	3.7		92.6	27.8	91.5	3.3	27.6
58	1.737	318	145	55	145	57	300	360	-12	140	4.5	3.7		55.1	44.6	69.4	18.5	3.8
59	1.734	328	150	235	235	146	280	-430	-210	15	4.5	3.7		52.0	79.4	87.2	25.6	3.4
60	1.774	338	192	280	191	275	450	-80	70	90	4.5	3.5		44.0	50.9	53.2	34.5	1.5
61	1.399	330	93	6	80	6	1675	-350	480	220	4.5	3.7		75.0	100.8	104.5	57.3	1.8
62	2.615	331	202	101	198	84	80	250	-60	70	4.5	3.7		108.9	96.0	114.4	94.1	1.2
63	2.124	330	324	50	51	325	-140	130	100	-7	4.4	3.7		39.0	67.1	74.3	24.5	3.0
64	2.252	323	146	55	144	60	290	210	-10	105	4.4	3.7		97.0	76.8	123.4	38.7	3.2
65	2.841	325	174	80	173	80	110	120	-35	55	4.4	3.7		95.5	94.9	143.4	18.5	7.8
66	3.018	329	178	109	105	184	70	150	50	-35	4.4	3.7		96.9	121.9	157.5	55.7	2.8
67	1.454	190	345	9	8	346	-200	-240	-30	-80	4.5	3.7		29.4	25.6	44.7	13.8	3.2
68	2.198	183	77	159	77	160	-90	50	140	40	4.5	3.8		41.0	92.8	117.9	21.9	5.4
69	1.768	181	160	70	171	75	80	-175	3	170	4.5	3.7		38.9	62.8	81.9	19.2	4.3
70	1.469	206	126	35	14	112	-105	-200	-100	170	4.4	3.6		31.7	26.0	48.1	18.9	2.5

N	R	BEAR	B1	B2	BR1	BR2	EX1	EY1	EX2	EY2	CUR1	CUR2	XL	R1	R2	R_{max}	R_{min}	RTO
71	2.070	190	274	201	184	270	75	110	0	-90	4.4	3.7	30	39.4	44.8	72.0	23.2	3.1
72	1.798	206	359	90	2	97	-100	-170	-115	80	4.4	3.6		48.1	33.6	66.5	30.8	2.2
73	2.277	207	14	58	16	58	-37	-45	-10	8	4.4	3.65		21.6	12.4	21.9	8.8	2.5
74	2.798	210	90	129	85	165	-30	-12	0	15	4.4	3.65		35.3	14.0	37.7	14.1	2.7
75	2.972	195	229	322	322	228	35	5	-30	-10	4.4	3.65		33.8	44.8	71.5	23.2	3.1
76	1.798	194	80	169	167	80	-130	72	65	120	4.4	3.7		34.0	41.6	65.6	20.2	3.2
77	2.332	194	200	218	194	213	80	100	0	-20	4.4	3.65		52.5	41.0	56.0	19.7	2.8
78	1.158	234	283	17	282	18	320	-35	-20	-620	4.4	3.7		28.0	21.1	36.8	20.2	1.8
79	1.554	225	170	185	170	185	7	30	140	170	4.4	3.7		16.4	21.2	22.2	2.9	7.7
80	1.216	254	263	168	279	175	85	-170	480	300	4.4	3.7		21.6	22.3	28.6	19.9	1.4
81	1.570	251	6	302	350	4	75	100	-30	-60	4.4	3.7		25.1	12.0	35.4	9.03	3.9
82	1.603	235	352	264	353	262	50	85	-100	80	4.4	3.7		21.5	13.4	28.6	13.3	2.1
83	0.396	253	72	87	86	72	-1725	-2300	12000	12000	4.6	3.5		24.2	13.5	25.8	2.3	11.1
84	0.732	248	318	194	184	270	900	140	2900	4000	4.4	3.6		37.9	12.9	42.5	12.9	3.3
85	1.015	213	130	233	230	144	-260	725	90	480	4.4	3.6		37.4	17.5	43.0	18.0	2.4
86	0.786	275	172	80	175	83	-875	140	-1150	-675	4.3	3.7		33.6	11.0	75.6	2.5	29.6
87	0.643	313	260	271	258	272	-2025	-1600	-900	-775	4.3	3.7		25.2	21.7	120.2	17.8	6.7
88	1.109	287	51	75	60	82	460	410	60	-120	4.3	3.7		33.5	18.9	32.7	10.1	3.2
89	1.414	272	342	245	348	230	140	-65	85	180	4.3	3.7		26.4	17.9	38.3	5.2	7.4
90	1.707	267	175	81	170	83	-100	35	0	-115	4.3	3.7		32.4	14.7	36.5	13.2	2.8
91	1.807	242	200	128	128	203	13	-65	5	80	4.3	3.7		24.6	13.0	34.5	11.5	3.0
92	1.911	231	97	174	175	95	-70	-15	65	-40	4.3	3.7		24.8	17.1	28.3	17.2	1.6
93	2.414	217	125	197	126	199	-25	15	10	13	4.3	3.7		21.1	7.5	31.7	6.2	5.1
94	2.012	216	7	265	6	231	-15	85	-45	55	4.4	3.7		30.5	16.3	33.1	15.4	2.1
95	1.783	284	139	205	138	192	-15	-155	-120	-90	4.4	3.75		44.4	21.8	46.1	18.5	2.5
96	2.286	305	81	173	82	173	190	-20	30	-40	4.4	3.75		69.0	27.1	80.0	19.2	4.2
97	2.012	297	352	295	357	311	100	-145	60	60	4.4	3.75		76.5	21.4	76.9	1.9	40.2
98	2.752	312	31	85	31	85	45	110	50	32	4.4	3.70		67.0	54.0	97.0	22.8	4.2
99	3.048	318	340	53	68	343	-45	35	30	45	4.4	3.70		45.3	88.2	114.3	2.5	45.5
100	2.347	314	175	281	180	276	15	-175	-60	-50	4.4	3.75		61.1	57.2	84.3	35.3	2.4
101	1.975	306	12	348	334	354	125	48	65	85	4.4	3.75		48.1	34.4	63.7	7.4	8.6
102	1.774	300	300	215	213	310	-175	-250	-65	40	4.4	3.75		55.6	16.7	60.1	1.2	48.9
103	1.518	284	286	190	286	175	-70	-180	100	-100	4.4	3.75		34.9	12.7	35.0	12.7	2.8

APPENDIX IV

TEMPERATURE STUDY FIELD DATA

N: Station number

R: Resistance (ohms)

T: Temperature (^{o}C)

N	R	T
1	972	25.8
2	920	27.3
3	1009	24.8
4	933	26.9
5	1007	24.8
6	961	26.1
7	943	26.6
8	889	28.2
9	979	25.6
10	977	25.6
11	959	26.1
12	1016	24.6
13	973	25.7
14	966	25.9
15	1015	24.6
16	1005	24.9
17	965	26.0
18	998	25.1
19	982	25.5
20	989	25.3
21	1027	24.3
22	978	25.6
23	999	25.0
24	993	25.2
25	988	25.3
26	998	25.0
27	988	25.3
28	1014	24.6
29	947	26.5
30	1022	24.4
31	984	25.4
32	945	26.5
33	958	26.2
34	949	26.4
35	953	26.3

N	R	T
36	952	26.3
37	955	26.2
38	921	27.2
39	983	25.5
40	950	26.4
41	977	25.6
42	966	25.9
43	970	25.8
44	954	26.3
45	971	25.8
46	947	26.5
47	952	26.3
48	970	25.8
49	971	25.8
50	959	26.1
51	1000	25.0
52	1010	24.7
53	961	26.1
54	951	26.4
55	975	25.7
56	960	26.1
57	989	25.3
58	1313	17.7
59	989	25.3
60	974	25.7
61	996	25.1
62	997	25.1
63	978	25.6
64	960	26.1
65	935	26.8
66	927	27.1
67	930	27.0
68	972	25.8
69	962	26.0
70	1022	24.4

APPENDIX V

SELF-POTENTIAL STUDY FIELD DATA

N: Station number

V: Potential drop along a 200 m line (millivolts)

V_C: Corrected value of V (after error distribution) (millivolts)

V_N: Potential drop between a station and the initial point with assumed zero potential (millivolts)

N	V	V_C	V_N	N	V	V_C	V_N
1	-23.9	-21.9	-21.9	34	3.8	5.8	-392.3
2	-33.4	-31.4	-53.3	35	-20.2	-18.2	-410.5
3	- 6.2	- 4.2	-57.5	36	-1.4	0.6	-225.5
4	- 7.9	- 5.9	-63.4	37	10.8	12.8	-214.7
5	-27.7	-25.7	-89.1	38	- 2.7	- 0.7	-215.4
6	24.5	26.5	-62.6	39	10.8	12.8	-202.6
7	-54.5	-52.7	-115.3	40	12.7	14.7	-187.9
8	- 2.9	- 0.9	-116.2	41	13.4	15.4	-172.5
9	-13.2	-11.2	-127.4	42	8.1	10.1	-162.4
10	-24.6	-22.6	-150.0	43	18.5	20.5	-141.9
11	8.0	10.0	-140.0	44	8.3	10.3	-131.6
12	-19.6	-17.6	-157.6	45	11.2	13.2	-118.4
13	- 4.7	- 2.7	-160.3	46	30.8	32.8	- 75.6
14	- 9.9	- 7.9	-168.2	47	-30.0	-28.0	-103.6
15	0.2	2.2	-166.0	48	- 1.0	1.0	-102.6
16	-12.8	-10.8	-176.8	49	43.2	45.2	- 67.4
17	- 8.1	- 6.1	-182.9	50	- 2.7	- 0.7	-258.0
18	- 7.7	- 5.7	-188.9	51	27.3	29.3	-228.7
19	-11.3	- 9.3	-197.9	52	-12.0	-10.0	-238.7
20	-31.0	-29.0	-226.9	53	6.8	8.8	-229.9
21	5.2	7.2	-219.7	54	1.6	3.6	-226.3
22	- 8.4	- 6.4	-226.1	55	0.8	2.8	-222.5
23	-32.2	-30.2	-256.3	56	- 0.8	1.2	-221.3
24	- 5.8	- 3.8	-260.1	57	10.6	12.6	-208.7
25	-16.1	-14.1	-274.2	58	-10.2	- 8.2	-216.9
26	- 4.8	- 2.8	-277	59	- 8.9	- 6.9	-223.8
27	- 1.5	0.5	-276.5	60	0.3	2.3	-221.5
28	- 7.8	- 5.8	-282.3	61	- 3.4	- 1.4	-222.9
29	-15.9	-13.9	-292.2	62	0.1	2.1	-220.8
30	-24.0	-22.0	-318.2	63	-19.0	-17.0	-237.8
31	-40.0	-38.0	-356.2	64	- 4.0	- 2.0	-239.8
32	-30.8	-28.8	-385.0	65	6.0	8.0	-231.8
33	-15.1	-13.1	-398.1				

SELECTED REFERENCES

Armstead, H. C. H., 1970, Utilization of steam and high enthalpy water (for electric power generation and other purposes): UN Symposium on the Development and Utilization of Geothermal Resources, Pisa, 1970, sec. IX.

Banwell, C. J., 1970, Geophysical techniques in geothermal exploration: UN Symposium on the Development and Utilization of Geothermal Resources, Pisa, 1970, sec. IV.

Dedkova, D., Halousek, J., Krcmar, B., and Prihoda, K., 1970, Geothermal prospection [illegible] shallow holes and its limitation: UN Symposium on the Development and Utilization of Geothermal Resources, Pisa, 1970, IV/5.

Djayadi, H., Pardyanto, L., and Alzwar, M., 1974, Possible energy sources in Indonesian volcanic areas: Geological Survey of Indonesia.

Einarsson, S. S., 1970, Utilization of low enthalpy water for space heating, industrial, agricultural and other uses: UN Symposium on the Development and Utilization of Geothermal Resources, Pisa, 1970, sec. X.

Facca, G., 1970, General report on the status of world geothermal development: UN Symposium on the Development and Utilization of Geothermal Resources, Pisa, 1970, sec. II.

Furgerson, R. B., 1970, A controlled-source telluric current technique and its application to structural investigations: Thesis 1313, Colo. School of Mines, Golden, Colo.

Furgerson, R. B., and Keller, G. V., 1974, Computed dipole resistivity effects for an earth model with vertical and lateral contrasts in resistivity: Report No. NR081275, Office of Naval Research, Washington, D.C.

Furumoto, A. S., Campbell, J. F., and Hussong, D. M., 1970, Seismic studies of subsurface structure in the Ewa coastal plain, Oahu, Hawaii: Pacific Sci., v. 24, no. 4, p. 529-541.

Furumoto, A. S., Wiebenga, W. A., Webb, J. P., and Sutton, G. H., 1973, Crustal structure of the Hawaiian Archipelago, Northern Melanesia, and the Central Pacific Basin by seismic refraction methods: Tectonophysics, v. 20, p. 153-164.

Furumoto, A. S., Woollard, G. P., Campbell, J. F., and Hussong, D. M., 1968, Variation in the thickness of the crust in the Hawaiian Archipelago, in The crust and upper mantle of the Pacific area: Geophysical Monograph 12, pp. 94-111, American Geophysical Union, Washington, D.C.

Grose, L. T., 1971, Geothermal energy: geology, exploration, and development (part 1): Colorado School of Mines Mineral Industries Bull., v. 14, no. 6.

Grose, L. T., and Keller, G. V., 1974, The Colorado School of Mines Nevada Geothermal Study - Report of Progress for the period May 1, 1974 to July 31, 1974: Colo. School of Mines, Golden, Colo.

Hochstein, M. P., and Hunt, T. M., 1970, Seismic, gravity, and magnetic studies, Broadlands Geothermal Field, New Zealand: UN Symposium on the Development and Utilization of Geothermal Resources, Pisa, 1970, IV/27.

Jordan, J. M., 1974, Geothermal investigations in the San Luis Valley, South-Central Colorado: Thesis 1478, Colo. School of Mines, Golden, Colo.

Keller, G. V., 1974, Drilling at the summit of Kilauea Volcano: Prepared for National Science Foundation, Colo. School of Mines, Golden, Colo.

__________ 1966, Dipole method for deep resistivity studies: Geophysics, v. 31, no. 6, p. 1088-1104.

__________ 1970, Induction methods in prospecting for hot water: Geothermics, spec. issue 2, p. 318-332.

Keller, G. V., and Frischknecht, F. C., 1966, Electrical methods in geophysical prospecting: Oxford, Pergamon Press.

MacDonald, G. A., and Abbott, A. T., 1970, Volcanoes in the sea, the geology of Hawaii: Honolulu Hawaii, University of Hawaii Press.

Malahoff, A., and Woollard, G. P., 1966, Geologic implications of magnetic surveys over the Hawaiian Islands: Pacific Sci., v. 20, no. 3, p. 265-311.

McEuen, R. B., 1970, Delineation of geothermal deposits by means of long-spacing resistivity and airborne magnetics: UN Symposium on the Development and Utilization of Geothermal Resources, Pisa, 1970, IV/22.

McNitt, J., 1970, The geologic environment of geothermal fields as a guide to exploration: UN Symposium on the Development and Utilization of Geothermal resources, Pisa, 1970, sec. 3.

Meidav, T., 1970, Application of electrical resistivity and gravity in deep geothermal exploration: UN Symposium on the Development and Utilization of Geothermal Resources, Pisa, 1970, IV/3.

Risk, G. F., MacDonald, W. J. P., and Dawson, G. B., 1970, D.C. resistivity surveys of the Broadlands Geothermal Region, New Zealand: UN Symposium on the Development and Utilization of Geothermal Resources, Pisa, 1970, IV/24.

Sestini, G., 1970, Heat-flow measurements in non-homogeneous terrains. Its application to geothermal areas: UN Symposium on the Development and Utilization of Geothermal Resources, Pisa, 1970, IV/17.

Stearns, H. T., 1966, Geology of the State of Hawaii: Palo Alto, Calif., Pacific Books.

Strange, W. E., Woollard, G. P., and Rose, J. C., 1965, An analysis of the gravity field over the Hawaiian Islands in terms of crustal structure: Pacific Sci., v. 19, no. 3, p. 381-389.

Strange, W. E., Machesky, L. F., and Woollard, G. P., 1965, A gravity survey of the Island of Oahu, Hawaii: Pacific Sci., v. 19, no. 3, p. 350-353.

Strangway, D. W., 1970, Geophysical exploration through geologic cover: UN Symposium on the Development and Utilization of Geothermal Resources, Pisa, 1970, IV/5.

Tongiorgi, E., 1970, Geothermal systems: UN Symposium on the Development and Utilization of Geothermal Resources, Pisa, 1970, sec. I.

Van Nostrand, R. G., and Cook, K. L., 1966, Interpretation of resistivity data: U.S. Geol. Survey Prof. Paper 499.

Zohdy, A. A. R., and Jackson, D. B., 1969, Application of deep electrical soundings for groundwater exploration in Hawaii: Geophysics, v. 34, no. 4, p. 584-600.